water

MDPI

Article

Multilayer Feedforward Artificial Neural Network Model to Forecast Florida Bay Salinity with Climate Change

Anteneh Z. Abiy [1], Ruscena P. Wiederholt [1,*], Gareth L. Lagerwall [1], Assefa M. Melesse [2] and Stephen E. Davis [1]

[1] The Everglades Foundation, 18001 Old Cutler Road, Suite 625, Palmetto Bay, FL 33157, USA
[2] Department of Earth and Environment, Florida International University, Miami, FL 33199, USA
* Correspondence: ruscenawiederholt@gmail.com

Abstract: Florida Bay is a large, subtropical estuary whose salinity varies from yearly and seasonal changes in rainfall and freshwater inflows. Water management changes during the 20th century led to a long-term reduction in inflows that increased mean salinity, and the frequency and severity of hypersalinity. Climate change may exacerbate salinity conditions in Florida Bay; however, future salinity conditions have not been adequately evaluated. Here, we employed a Multilayer Feedforward Artificial Neural Network model to develop baseline salinity models for nearshore and offshore sites. Then, we examined the impacts of climate change on salinity using forecasted changes in various input variables under two climate change scenarios, representative concentration pathways (RCP) 4.5 and 8.5. Salinity could rise by 30% and 70% under the RCP4.5 and RCP8.5 forecasts, respectively. Climate change affected nearshore salinity significantly more, which rapidly fluctuated between mesohaline (5 to 18 PSU) and metahaline (40 to 55 PSU) to hypersaline conditions (>55 PSU). Offshore salinities ranged between euhaline (30 to 40 PSU) to metahaline (40 to 55 PSU) conditions. Our study suggests that increased freshwater flow would help maintain suitable estuarine conditions in Florida Bay during climate change, while our novel modeling approach can guide further Everglades restoration efforts.

Keywords: Florida Bay; climate change; Everglades; artificial neural networks; data modeling; salinity forecasting

Citation: Abiy, A.Z.; Wiederholt, R.P.; Lagerwall, G.L.; Melesse, A.M.; Davis, S.E. Multilayer Feedforward Artificial Neural Network Model to Forecast Florida Bay Salinity with Climate Change. *Water* **2022**, *14*, 3495. https://doi.org/10.3390/w14213495

Academic Editors: Zhenxin Bao and Guangyuan Kan

Received: 30 September 2022
Accepted: 28 October 2022
Published: 1 November 2022

1. Introduction

The health of global estuaries is increasingly compromised by highly variable, persistent, and extreme salinity conditions [1–6]. Salinity is a fundamental estuarine characteristic that affects the health, water chemistry, and habitat suitability of this ecosystem [7]. Different salinity levels also affect the composition and spatial distribution of plant communities and most animal species in estuaries [8]. Studies of 55 estuaries in the western U.S. indicated that up to 85% of vegetated tidal wetlands have been lost due to multiple causes including sea level rise, decreasing freshwater inflow, and other factors over the past few decades [9]. Climate change and changes in freshwater inflow are principal factors of these ongoing global challenges in estuaries. Climate change will likely continue to adversely affect estuaries via sea level rise, extreme hydrological conditions, and increased evaporation. However, estuaries are critical ecosystems, serving as a buffer between oceanic tides and freshwater bodies, and providing habitat for fish, invertebrates, and migratory birds, which supply economic and ecological benefits [3,5,10]. Understanding how these changes will alter an estuarine salinity regime can help inform management efforts.

Florida Bay, a subtropical estuary within Everglades National Park, is part of the Greater Everglades ecosystem, home to numerous iconic species, and designated as a World Heritage Natural Site [11]. Historically, the bay has provided habitat for American crocodiles *Crocodylus acutus*, West Indian manatees *Trichechus manatus*, and roseate spoonbills *Platalea ajaja*. The bay is characterized by a small tidal range, from 0.2 to 0.6 m, and

receives freshwater inflow from rainfall, sheet flow from the Everglades, and potential groundwater discharge. Over the last century, freshwater inflows from the Everglades have been greatly reduced by drainage and altered hydrology [12]. Biological and statistical estimates indicated that the net historical flow into the bay would have been four times greater than current values and that the water levels in the bay could have been 15 cm higher than current levels [13–15]. In addition, water management practices have decreased inflows from Taylor Slough, a direct freshwater inflow source for Florida Bay [16]. Florida Bay's bottom is characterized by a series of shallow mud banks, which limit water exchange among various basins across the bay [17]. Combined with reduced inflows, this limited exchange promotes the development of hypersaline conditions in several of the bay's interior basins [18] making them vulnerable to large scale seagrass die-offs [19,20]. Seagrass wasting disease, caused by the slime mold (*Labyrinthula* species), is also more common at these high salinity levels [21].

Multiple factors influence salinities in estuaries including temperature, evaporation, rainfall, freshwater flow, and sea level rise. However, water management has also affected long-term salinity patterns in Florida Bay [8]. Following seasonal patterns, estuarine salinities can vary between nearly freshwater (oligohaline, 0.5 to 5 PSU) to hypersaline conditions (>55 PSU). In addition to surface water inflow, the balance between rainfall and evaporation losses is known to affect the salinity of Florida Bay [18]. The incidence of hypersaline conditions creates unfavorable conditions for the survival of flora and fauna that estuaries harbor [22,23]. Climate change induced alterations in rainfall patterns, combined with increases in temperature, can lead to higher evaporation losses. However, forecasted climate data show an increase in precipitation, meaning surface water flows are likely to increase. Nevertheless, the combined effect of these variables on salinity in Florida Bay has not been well established in previous studies.

Understanding the impacts of climate change on the salinity of estuaries like Florida Bay is critical for guiding water management strategies, protecting important estuarine habitats like seagrass, and informing ecosystem restoration efforts. In fact, Florida Bay salinity is a performance measure used to guide project and operational planning associated with the Comprehensive Everglades Restoration Plan [18,24–26]. Forecasting future hydrologic conditions using projected meteorological variables in the Everglades system is an important first step in evaluating the impacts of climate change on Florida Bay's salinity. Climate change in South Florida will likely result in warmer temperatures, shifts in seasonal rainfall patterns, and changes in rainfall distribution (Infanti and Kirtman 2019). These changes will likely alter the timing and volume of freshwater flow into Florida Bay. In addition to alterations in freshwater inflow, changes in potential evapotranspiration (ETP) and sea level will also impact salinity levels in Florida Bay. According to the Southeast Florida Regional Climate Change Compact Sea Level Rise Work Group (Compact), the mean sea level at the Key West tide gauge by 2040 is projected to increase by 25.4 to 43.18 cm relative to 2000 levels (0 cm; referencing the NOAA Intermediate High projecting curve) [27]. Indeed, from 2000 to 2020, the mean annual sea level at Key West (with regular seasonal fluctuations from coastal ocean temperatures, salinity, wind, atmospheric pressure, and ocean currents removed) has risen by 11.51 cm (https://tidesandcurrents.noaa.gov/sltrends/sltrends_station.shtml?id=8724580 (accessed on 10 December 2021)). By 2060, the sea level around Florida Bay could increase by 35.6 to 86.4 cm.

A few tools already exist to predict salinity in Florida Bay [15,28–31]. For instance, a spatially explicit mass balance model for Florida Bay, FATHOM, was used to predict salinity under increased freshwater flows [29]. Salinities decreased under modest increases of freshwater flow for the north, northeastern, and eastern regions of the bay, while the western regions were insensitive to even large increases in freshwater flow. As freshwater flow increases, the composition of the seagrass community was also predicted to change to a state closer to that observed historically. FATHOM was also altered to predict changes in salinity under climate change as part of a study of juvenile fish habitat suitability [28,32]. The

study increased sea level (by 45.7 cm) and ETP rate (differences due to a 1 °C temperature increase), and both increased and decreased levels of rainfall (±10%) and runoff (±5%) to the bay. While the overall predicted change in salinity was small, sea level rise increased salinity the most. Alterations in ETP, rainfall, and runoff resulted in smaller changes in salinity [32]. Under a climate change scenario for 2060 with a 1.5 °C temperature increase, associated increases in ETP, and 1.5 feet of sea level rise, salinity in Florida Bay is predicted to change little if the accretion rates of the bay's mudbanks continue to keep pace with 1.5 feet of sea level rise. However, if mud banks do not keep pace with sea level rise, then estuarine habitat is predicted to be lost in the bay [33].

These available tools for salinity prediction presented difficulties in implementation or had different time periods of simulation. Given our need to simulate changes in specific variables under scenarios of climate change, we developed a new modeling tool to estimate salinity in Florida Bay using artificial neural networks (ANN). The effectiveness of ANN in a hydrological system's evaluation is quite robust, particularly when time series data analysis and forecasting is involved [34]. Compared to other hydrological modeling tools, the American Society of Civil Engineers found neural networks to have great potential in hydrological modeling and forecasting [35,36], and ANN modeling has been used for studies of water quality assessment, flow and flood forecasting, and rainfall and drought forecasting [37–40].

Our objectives were (1) to develop models simulating salinity in six different sites across Florida Bay using pertinent factors influenced by a suite of climatic and hydrologic drivers in the Everglades, and (2) to assess how future (2030 to 2051) salinity conditions will vary under a changing climate. We developed a baseline Feed Forward Artificial Neural Network model for each site using daily records from 2000 to 2021. We established both hydrological and statistical criteria to select the input variables for the ANN models with three categories: (1) hydrological criteria, (2) correlations between each pair of input variables, and (3) impact factors determined by random forest classifications assessing the relative weight of each candidate variable. The baseline model was then used to simulate future Florida Bay salinities in response to climate change using two Representative Concentration Pathways (RCP), RCP4.5 and RCP8.5 scenarios [41,42]. Our results can be used to guide decisions for upstream Everglades restoration that would improve inflows and maintain the estuarine health of Florida Bay in the face of climate change.

Florida Bay Study Sites

Florida Bay is a shallow estuary encompassing 2200 square kilometers between the tip of the Florida mainland and the Florida Keys (Figure 1). The bay is characterized by a microtidal estuary where wind-forcing is as important if not more important in controlling water level variation than tidal forcing [22]. The average depth of the bay is about one meter, allowing for a dominance of seagrasses that provide habitat for many species and are also a source of primary productivity [22,43]. The bay can be divided into three zones: a western zone with extensive mudbanks and relatively stable marine conditions, a central zone with basins that exhibit a tendency for hypersaline conditions, and an eastern zone with highly variable salinity [44]. We selected six sampling sites, representing distinct hydrologic basins, and paired as three nearshore and three offshore bay sites. Moving from nearshore to offshore, our transects included Murray Key (MK) to Johnson Key (JK); Garfield Bight (GB) to Buoy Key (BK); and Terrapin Bay (TB) to Whipray Basin (WB, Figure 1). These sites are vulnerable to hypersalinity, as they are distal from the two primary overland freshwater sources, Taylor, and Shark River Slough.

In general, salinity across the bay also varies seasonally, with hypersalinity usually occurring during summer and estuarine salinities occurring in the fall and winter [25]. A delay in the onset of the wet season can lead to pronounced hypersaline events (>55 psu), which can lead to significant ecological impacts [22]. South Florida is characterized by a sub-tropical hydrologic regime with a wet season (roughly, May to October) dominated by localized convective rainfall, tropical depressions, thunderstorms, and hurricanes. The

area receives 1100 to 1500 mm of rainfall per year, of which more than 70% is received in the summer [45]. Annual ETP is of about the same magnitude as precipitation and usually peaks in late spring or early summer [18,22,43]. Salinity variability in Florida Bay follows a seasonal pattern in Southeast Florida (Figure 2). Often, the evaporation loss during the dry season is much greater than the rainfall, so salinity gradually increases in the bay (January to May). The difference between rainfall and ETP is greatest during April, but the peak salinity for both nearshore and offshore regions of the bay occurs in May—before the onset of the wet season. The salinity starts decreasing in June, when rainfall significantly exceeds ETP.

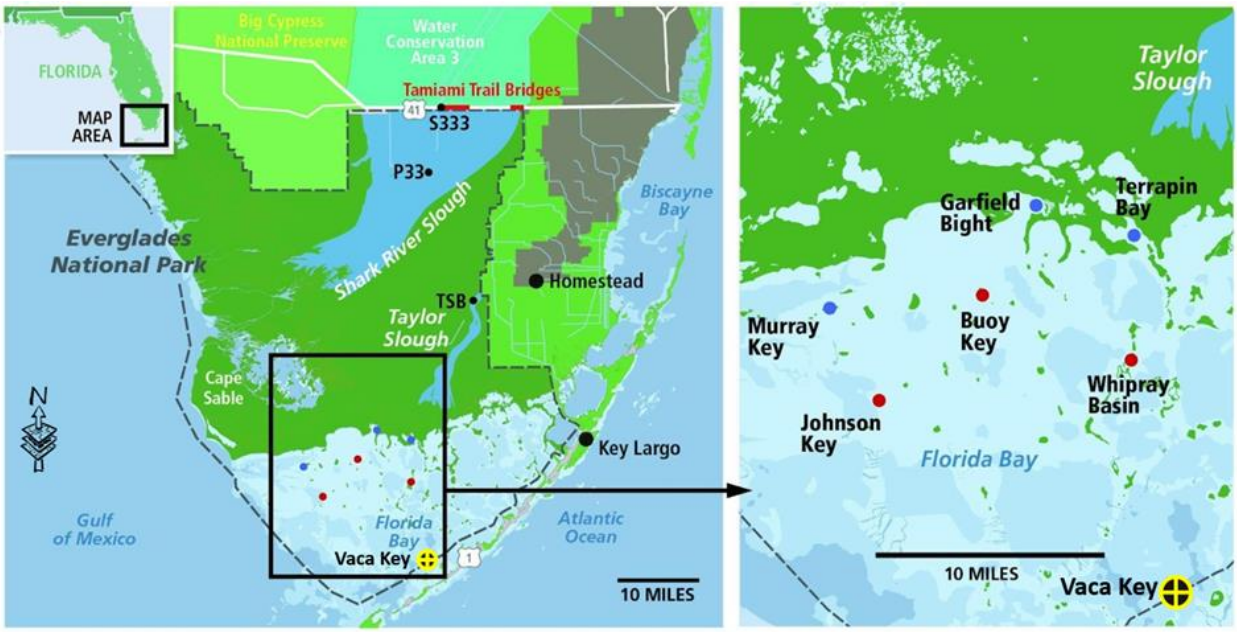

Figure 1. Map showing the location of Florida Bay at the tip of the Florida Peninsula and the locations of stage (P33 and Taylor Slough Bridge TSB) and flow sampling (S333) stations in the Everglades (left panel). The location of study transects Murray Key (MK) to Johnson Key (JK); Garfield Bight (GB) to Buoy Key (BK); and Terrapin Bay (TB) to Whipray Basin (WB) are identified (right panel). Nearshore sites are marked in blue, while offshore sites are marked in red. The tidal data was collected at the NOAA sea level monitoring station (ID 8723970) at Vaca Key.

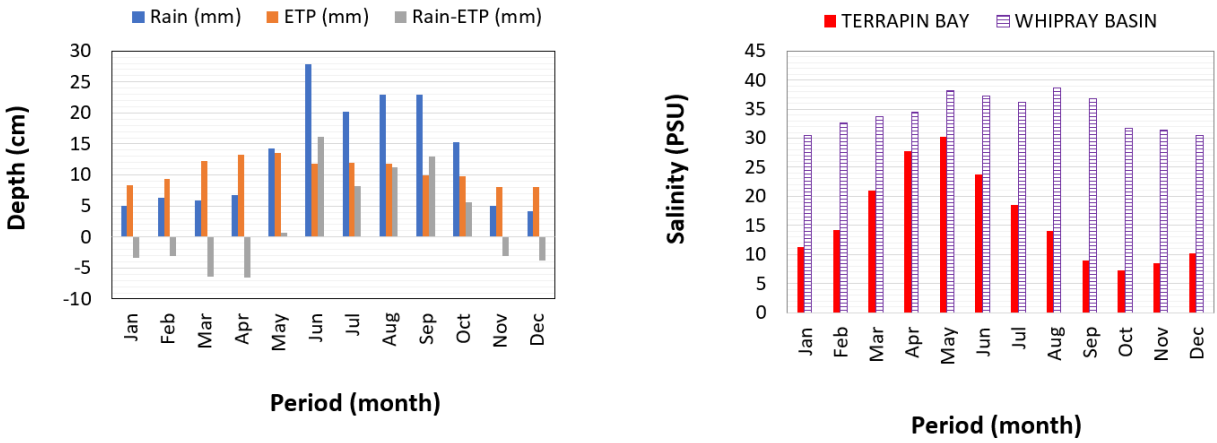

Figure 2. Monthly mean rainfall, evapotranspiration (ETP), and the difference between the two (**left**). Monthly mean salinity in Terrapin Bay and Whipray Basin, illustrating seasonal and spatial variability in bay salinities (**right**).

2. Materials and Methods

2.1. Baseline Data Sources

We used data from the South Florida Water Management District's (SFWMD) environmental database, DBHydro (https://www.sfwmd.gov/science-data/dbhydro (accessed on 10 December 2021)). Variables included: daily mean salinity (PSU), daily mean stage, daily mean flow daily total rainfall, daily mean potential evapotranspiration (ETP), and daily mean air temperatures. The data was collected by different institutions using different methodologies such as the National Park Service and Florida International University. However, the SFWMD reports salinity as quality-controlled data in Practical Salinity Units (PSU), so to be consistent, we referred to salinity in PSU in this manuscript. Salinity, stage, and rainfall data were gathered at each site, while ETP and air temperatures were based on a regional mean. ETP data were derived from Joe Bay (JBTS) and Everglades stations, S331W and 3AS3WX. These data were used to develop a representative regional ETP record. Likewise, air temperatures from each of the sites were used to calculate a representative, regional air temperature record. Daily mean sea level at Vaca Key was obtained from the National Oceanic and Atmospheric Administration's Tides and Currents database (https://tidesandcurrents.noaa.gov/map/index.html?region=Florida (accessed on 10 December 2021)).

2.2. Forecasted Data Sources

This study used future climate projection data from multiple Global Circulation Models (GCMs) used in the Coupled Model Intercomparison Project Phase 5 (CMIP5) for the RCP 4.5 (stabilization without overshooting to 4.5 W/m^2 by 2100) and RCP 8.5 (increasing radiative forcing to 8.5 W/m^2 by 2100) scenarios. We used localized constructed analogs (LOCA) downscaled data [46] from 27 GCMs that were available daily and in 1/16th degree grid resolution. These datasets can be downloaded publicly from Lawrence Livermore National Laboratory (https://gdo-dcp.ucllnl.org/downscaled_cmip_projections/dcpInterface.html (accessed on 10 December 2021)). Specifically, LOCA data were found to be suitable for hydrological simulations because they produce better estimates of extreme days than other commonly used bias corrected constructed analog methods [46]. We extracted LOCA datasets for the South Florida region including precipitation and minimum and maximum temperature from 1950 to 2099.

We also needed additional climate variables such as solar radiation, wind speed, and humidity to estimate ETP. Since LOCA downscaled data were not available for these variables, we derived them from a combination of GCMs and Regional Climate Models (RCMs). We used the Coordinated Regional Climate Downscaling Experiment (CORDEX) initiative (https://cordex.org/data-access/how-to-access-the-data/ (accessed on 10 December 2021)), a program sponsored by the World Climate Research Program (WCRP), for additional future projected data required to estimate ETP. Previous studies used RCMs' data for the state of Florida [47,48].

In this study, we used the Penman-Monteith (P-M) equation, a widely used method in regional hydrological analysis, to estimate potential evapotranspiration (ETP) [49,50]. P-M methods require several climate variables such as solar radiation, surface temperature, wind, and humidity. The surface temperature data were available from the LOCA downscaled data, while the remaining variables were obtained from the dynamically downscaled data from the RCMs. In spite of this record, the presence of ETP availability and uncertainties in Florida Bay are reported [51].

2.3. Description of Baseline and Forecasted Input Variables

Rainfall in South Florida is skewed with the wet season occurring between late May to early October [45,52]. We discerned the same regional pattern in the observed rainfall data in Florida Bay during the study period of 2000 to 2021. Over this study period, the observed annual average rainfall in Florida Bay was 1356.36 mm. The RCP4.5 and RCP 8.5 scenarios exhibited little difference in forecasted rainfall from 2030 to 2051, with an

annual average of 1320.8 and 1270 mm, respectively. The forecasted rainfall dataset under the RCP4.5 and RCP8.5 scenarios (Figure 3) represented the seasonal variability in the area; however, both scenarios suffer from ensembling effects.

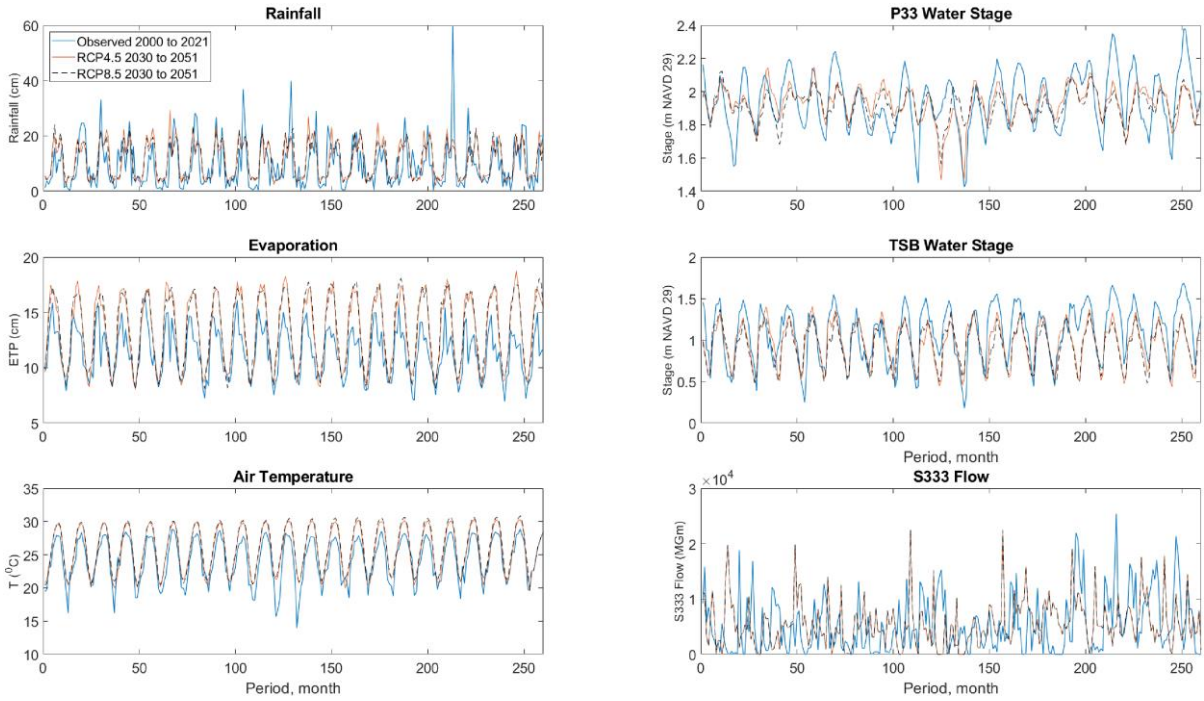

Figure 3. Monthly aggregated observations (2000 to 2021) and forecasted (2030 to 2051) datasets used in this study. The observed datasets were used to develop the FF-ANN model that produced the baseline models. After the models were deemed satisfactory, they were used with forecasted climate change and hydrological data were used to simulate the future coastal salinity changes.

The observed temperature was in the range of 14.0 to 29 °C. However, the forecasted temperature indicates an increase in range from 19.6 °C to 31.0 °C. The forecasted ETP was estimated to increase up to a total annual average of more than 1524 mm compared to the historic record of 1371.6 mm. The representation of hydrological conditions and future changes in the face of climate change were evaluated using the observed and modeled water levels at the Shark River Slough station P33 and the Taylor Slough station TSB, and Shark River Slough flows at S333. The baseline stages at the P33 and TSB stations, which were correlated with each other, were characterized by seasonal fluctuations following the typical wet and dry season cycles (Figure 3). However, the representative flow into the ENP is the result of flow regulations that are driven by water demand.

We used the daily mean sea level data at Vaca Key recorded over the study period (Figure 4A), representing a sequential time series plot where the average daily high and low tide are depicted as the peaks and troughs respectively. The raw mean sea level data was disaggregated into two frequency components using a simple convolution filtering over a 60-day moving window (Figure 4B,C). After testing the raw and filtered mean sea level datasets, the use of the low frequency signal was found to be most useful in our final models. The low frequency filtered dataset represented the seasonal and trend components of the mean sea level, whereas the high frequency dataset, composed primarily of the daily tidal fluctuation, was the difference between the observed mean sea level and the low frequency filtered datasets. The numeric values of these two datasets can be changed by adjusting the moving window size. However, after some experimentation, we found that a 60-day moving window was a reasonable assumption. As indicated in the supplementary material Figures S1 and S2, the mean annual tidal fluctuations encompass the daily tidal

fluctuations with the observed data having a least square trend line slope of 0.0019 m and the projected sea level rise having slope of 0.013 m.

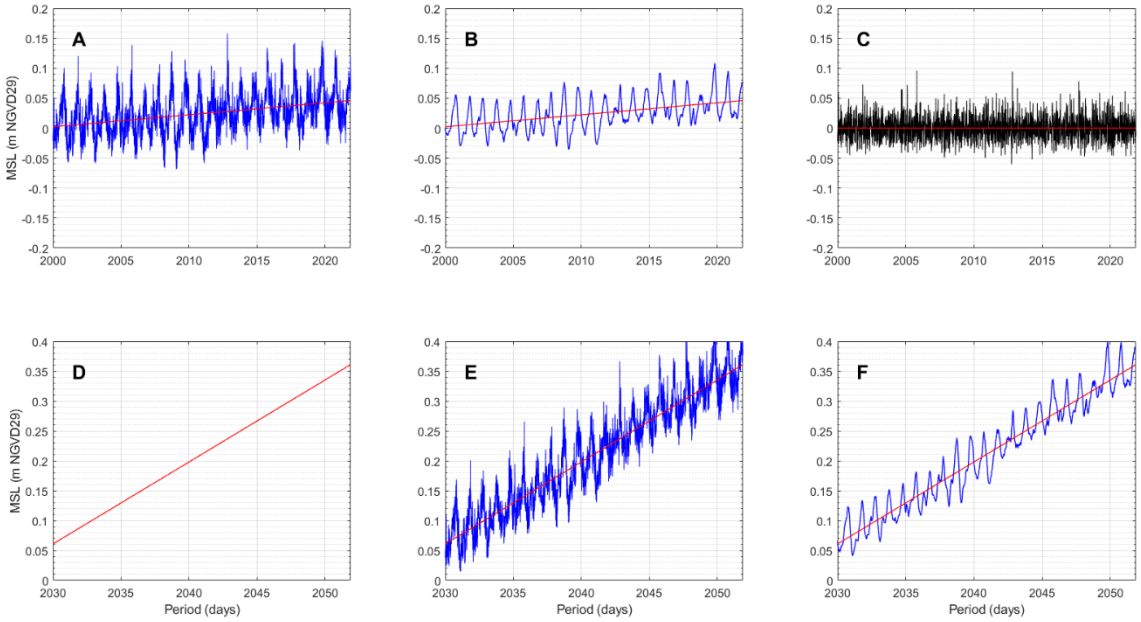

Figure 4. The observed tidal fluctuation data (**A**) was filtered using convolution (smoothing) to generate the low frequency that combines the seasonal and trend components of the observed sea level rise data (**B**). The difference between the observed mean sea level (**A**) and smoothed dataset (**B**) is plotted in daily tidal fluctuations (**C**). The low pass, smoothed data (**B**) was used to generate the baseline model. Furthermore, the sea level rise trend from the NOAA intermediate high forecast (**D**) was used to predict the sea level rise (**E**). The forecasted sea level rise data (**E**) is smoothed in the same manner as the observed dataset to generate the input used in simulating future salinity forecasts (**F**). The blue lines show the tidal data, the red lines are the linear trends of the corresponding data sets, and the black lines refer to the residual tidal data from the low pass, smoothed results.

The sea level rise forecast was conducted using the NOAA intermediate high forecast rate [53,54]. This sea level forecast rate was recommended for intermediate time ranges (up to 2070) by the Southeast Florida Regional Climate Change Compact Sea Level Rise Work Group [27]. Although the long-term forecast follows an exponential formulation, for a short-term forecast between 2030 and 2051, we considered a linear rate reasonable. Therefore, we calculated the slope of the segment for this period and developed a slope intercept equation to forecast a linear trend of future sea level rise. To capture the unknown tidal fluctuations, we added the daily fluctuations observed in the observed data (Figure 4C). We then used the low frequency component of the forecasted mean sea level, which we assumed to be a better representation of the near-term sea-level rise forecast. In this study, we used only one forecasted sea level rise scenario for both the RCP4.5 and RCP8.5 climate change scenarios.

2.4. Hydrologic Data Sources

The regional hydrologic conditions of South Florida in response to future climate projection data was simulated using the South Florida Water Management Model (SFWMM) version 6.5.5. This regional scale physically based hydrologic model simulates coupled movement and distribution of surface water and groundwater flow (South Florida Water Management District, 2005). The model also simulates canal networks, hydraulic structures, levee seepage, reservoirs, well pumping, and other operational rules and conditions of the Central and South Florida Project. The SFWMM used time series climatic data for 41 years (1965–2005). The SFWMM has been widely applied for water management and

restoration planning and assessment in South Florida [55,56]. We simulated RCP4.5 and RCP8.5 scenarios for near-term (2016–2056) and long-term (2059–2099) periods for existing infrastructure and operations.

2.5. Input Variable Selection

While more than 20 candidate variables were tested, the final ANN models used only seven input variables. We used three criteria to identify these final variables, including correlations among input variables, relative weights of input variables, hydrological representations of Shark River Slough and Taylor Slough, and atmospheric and sea level conditions. First, a larger set of independent variables was used to evaluate the correlation between variables. For the variable correlation test we gauged variable importance based on *t*-statistics (Figure 5). Among the candidate variables, those with lower correlations were selected for further evaluation using the relative weights and hydrological considerations.

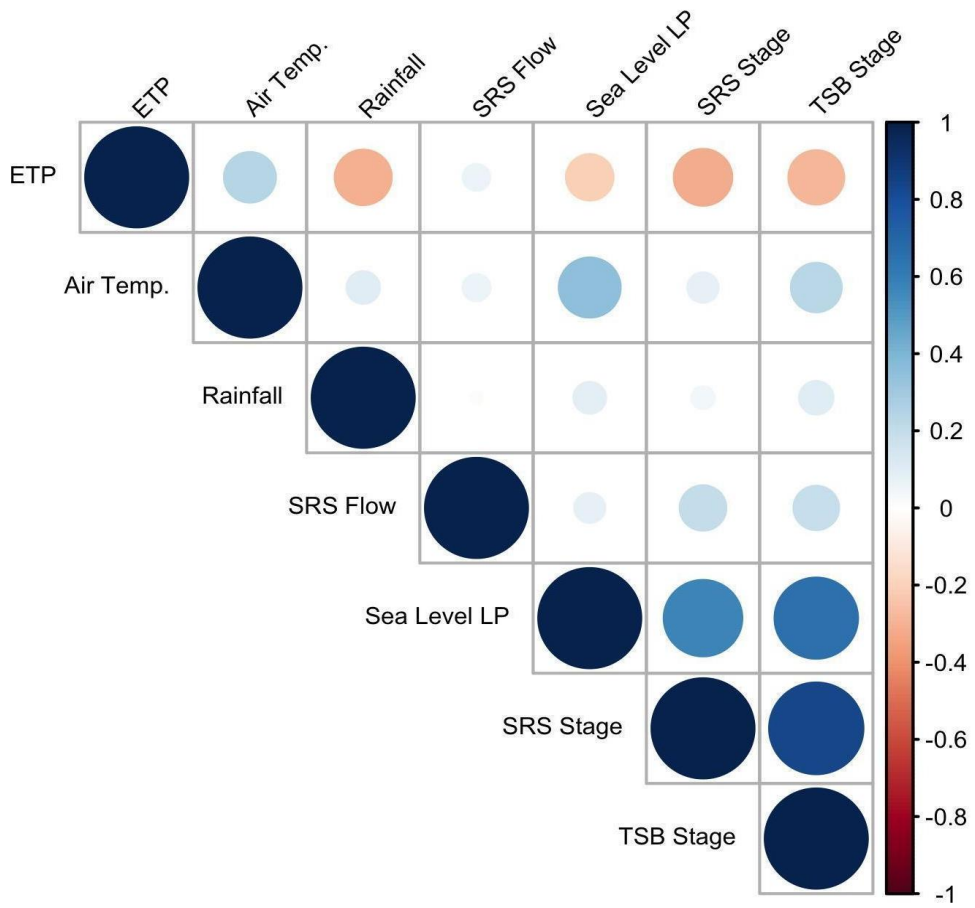

Figure 5. Correlation plot for input variables. Variables were daily mean values except for the daily sums of rainfall. SRS Stage was measured at the P33 station in Shark River Slough, TSB Stage was measured at the Taylor Slough Bridge station in Taylor Slough, SRS Flow was measured at the S333 station in Shark River Slough, and the Sea Level LP was measured at Vaca Key using a low pass filter.

The second model variable selection criteria were based on the relative weight of each independent variable in predicting salinity, which was conducted using a random forest classification algorithm consisting of 100 decision trees. This algorithm, implemented in the JMP suite, calculated the values for the contributions, portions, and ranks that came from the aggregated results from the number of trees–100 in our study. For the ease of calculation, speed, and reliability, we used the default of 100 trees. The variables' weights are given below (Table 1). Details of the random forest algorithm implementation for input variable analysis in JMP is given in [57].

Table 1. Input variable analysis results showing the relative weights of the observed input variables in predicting the observed salinities for each study site. Color codes show the weights of the variables for each site; blue refers to relatively higher weights, white refers to intermediate weights, and red refers to lower weights. The actual weights are given as percentages.

Predictor	JK	MK	BK	GB	TB	WB
P33 Stage	36%	33%	38%	41%	46%	25%
TSB Stage	20%	21%	25%	32%	21%	17%
Air Temperature (°C)	19%	22%	11%	9%	11%	34%
ETP	12%	14%	13%	8%	13%	13%
S333 Flow	6%	4%	6%	2%	3%	5%
Mean Sea Level	6%	4%	6%	7%	5%	4%
Rain	2%	2%	1%	1%	1%	2%

Third, we attempted to represent the two major sloughs (Shark River Slough and Taylor Slough) in both flow and water levels. Water level measurements in both Shark River Slough and Taylor Slough in these sub-basins have some level of correlation; however, to incorporate current and any future potential flow management activities, we decided that both local sub-basins should have a hydrological representation. Therefore, stages recorded at the P33 station in Shark River Slough, and the Taylor Slough Bridge station (TSB) in Taylor Slough were used as input variables for this modeling protocol. In addition, the hydrology of the Everglades was represented using a representative flow rate record at the S333 station in Shark River Slough. We did not include flow measurements in Taylor Slough because of a high correlation between the sub-basins, and because of intermittently missing values in flow measurements in the Taylor Slough. For the flow and stage data, we tested a variety of lags including 3 and 8 days, and 1, 2 and 3 weeks, and mean flow or stage values over the past week or past 2 weeks. Finally, input variables like wind speed and direction, and daily tidal mixing were tested but had a lower than 1% predictive potential, so we did not include these parameters in the ANN model.

2.6. Artificial Neural Network Modeling Formulation

Feed-Forward Artificial Neural Networks (FF-ANN) are part of the supervised artificial intelligence training models that formulate a protocol to input known variables (X_1, X_2, X_3, . . . , X_n) and produce a desired output (Y_m). As part of supervised learning algorithms, multilayer feedforward artificial neural network modeling protocols provide a simplified architecture that is easy to replicate. The robustness of the modeling protocol, as well as the final model result, allows FF-ANN models to assess the system under consideration by changing the input variables. Because FF-ANN models pass input variables forward through the activation functions to generate an expected output, they are intuitive for assessing the response of the outputs due to changes in one or multiple input variables [58–60]. Aside from their simplicity and replicability, other modeling techniques such as gene-expression programming, evolutionary polynomial regressions, model trees, and support vector machine models are valuable tools for water resource and water quality studies [61–63].

While both the dependent and independent variables are known, the FF-ANN model training generates a series of algorithms based on a least square objective function [64,65]. The FF-ANN model is known for its advantages in effectively modeling relationships between dependent and independent variables while providing robust and replicable model output that can be used for further studies, and the model evaluation in different scenarios [64,66]. The structure of neural networks contains the input (independent variable), hidden (activation function), and output (dependent variable) layers [35,36,64,67]. A hidden layer can contain several neurons *(i)* that solve the relative weight of each independent variable (X). In a FF-ANN, each input variable (X) from the input layer is weighted at every

perceptron by an activation function. The output from a neuron is provided as a linear equation given as:

$$Y_{i,\,j} = \varphi(\sum_{i\,,\,j=1}^{n} X_{i,\,j} + b_{i,\;\,j}) \tag{1}$$

where the activation function is the linear equation output from neuron i and the independent variable j, X are the independent variables given as $X = (X_1, X_2, \ldots\ X_j)$, φ the weight of the independent variable $X_{i,\,j}$ in the ith neuron, and $b_{i,j}$ is the bias coefficient for the independent variable $X_{i,\,j}$ in the ith neuron.

Depending on the number of hidden layers, one or more types of activation functions can be deployed. There are several activation functions *(f)* that can be used in a FF-ANN. Among others, the hyperbolic tangent function provided an advantage for capturing the time series oscillations through its fundamental assumption of an asymmetric data distribution scaled from 1 to −1 [68]. The mathematical formula for the hyperbolic tangent function is:

$$\varphi\left(X_{i,\;\,j}\right) = tanh\,(x) = \frac{2}{1+e^{-2x}} - 1 \tag{2}$$

In this study we have deployed a three-layer FF-ANN model. The first layer is the input variables container. For an i number of neurons in a single hidden layer, and j number of input variables the FF-ANN model output from each neuron (Y_i) within the second layer (the hidden layer) has a mathematical formulation of:

$$\begin{aligned} Y_1 &= tanh\left(0.5 * \left(\beta_{1,1}X_{1,1} + \beta_{1,2}X_{1,2} + \cdots \beta_{1,j}X_{1,j} + \epsilon\right)\right. \\ Y_2 &= tanh\left(0.5 * \left(\beta_{2,1}X_{2,1} + \beta_{2,2}X_{2,2} + \cdots \beta_{2,j}X_{2,j} + \epsilon\right)\right. \\ Y_i &= tanh\left(0.5 * \left(\beta_{i,1}X_{i,1} + \beta_{i,2}X_{i,2} + \cdots \beta_{i,j}X_{i,j} + \epsilon\right)\right. \end{aligned} \tag{3}$$

Each of the outputs (Y_i) from the individual neurons in the hidden layer are integrated in the final algorithm that estimates the predicted values for the dependent variable as:

$$Salinity = \sum_{i=1}^{n} \omega_i Y_i + \varepsilon \tag{4}$$

The weights of each of the individual neuron's outputs are defined by considering a least square minimum objective function that evaluates the model outputs (or predictions) with the primarily sampled validation datasets of the target variable. In this study, we have observed the correlation coefficient and root mean square error between the observed and prediction salinities.

The ANN was simulated using more than 7000 matching observation points where one third of the data was held back for model validations. The model implementation follows a two-step process. The neural network is designed to randomly sample two thirds of datasets for model training while holding back the remainder one third for model validation. Because we decided to apply a single hidden layer model, we ran the neural network iteratively by increasing the number of hidden nodes until an acceptable objective function was achieved. We assessed how well our models predicted salinity using R^2 values, RMSE between predicted and actual salinity values, and residual analysis to help assess the error distributions. After the model's performance was deemed acceptable, we extracted the background algorithm to evaluate climate change effects on Florida Bay salinity. The details of neural network modeling including the evaluations during training, validation as well how the back propagation algorithm functions are given in [57].

We ran artificial neural networks in JMP 14.3.0 of SAS Institute Inc. [57]. Furthermore, we have developed a post processing script for both Matlab and R users that are included as Supplementary material in this manuscript. Our models were used to forecast salinity (from 2030 to 2051) under future climate change conditions for both the RCP4.5 and RCP8.5 scenarios.

2.7. Coastal Salinity Index

To characterize the salinity data, we used a coastal salinity index that characterizes drought and freshwater conditions in coastal waters. The Coastal Salinity Index (CSI) is similar to the Standardized Precipitation Index. In the CSI, monthly mean salinity data are standardized to have a mean of zero and a standard deviation of one. Negative values are the number of standard deviations below the mean and represent increasing saline conditions (coastal drought CD; Table S1). Positive values are the number of standard deviations above the mean and represent increasing freshwater conditions [69–71]. The index represents changes in monthly salinity conditions with respect to average conditions at a site. We used the CSI package in R [69–71].

3. Results

3.1. Climate Forecast and Hydrological Modeling Results

An ANOVA revealed significant differences between the three scenarios for air temperatures, ETP, rainfall, stage, and flow data. A post hoc Tukey test using a Bonferroni correction [72–74] revealed that daily air temperatures varied significantly among all three scenarios (RCP4.5 vs. Observed 1.47 °C, RCP8.5 vs. Observed 1.77 °C, RCP8.5 vs. RCP4.5 0.31 °C, p-value < 0.0001), between the observed data and the two climate change scenarios for daily ETP (RCP4.5 vs. Observed 0.03 inches, RCP8.5 vs. Observed 0.03 inches, p-value < 0.0001), and between the observed data and the RCP4.5 scenario for daily total rainfall (RCP4.5 vs. Observed 0.02 inches, p-value < 0.012). Daily stage data at P33 varied significantly among all three scenarios (RCP4.5 vs. Observed −0.05 feet, RCP8.5 vs. Observed −0.09 feet, RCP8.5 vs. RCP4.5 −0.04 feet, p-value < 0.0001), as it did for Taylor Slough Bridge (RCP4.5 vs. Observed −0.39 feet, RCP8.5 vs. Observed −0.47 feet, RCP8.5 vs. RCP4.5 −0.07 feet, p-value < 0.0001). Daily flow data from S333 varied between the observed data and the two climate change scenarios (RCP4.5 vs. Observed 15.92 cubic feet per second, RCP8.5 vs. Observed 15.92 cubic feet per second, p-value < 0.011). Even though some of the variables were not statistically significantly different between scenarios, since the objective of this work was to develop a model based on the observed data and to generate an understanding of how salinity in Florida Bay could change with climate change, we decided to use the available forecasted data.

In Florida Bay, the mean annual rainfall from 2000 to 2021 was 44.5 inches. However, our climate downscaling for the period of 2030 to 2051 predicted a mean annual rainfall of 51.8 inches and 51.3 inches for RCP4.5 and RCP8.5 scenarios, respectively. The observed daily rainfall had a significant seasonal and interannual variability that also represented the incidence of tropical storms. However, such extreme variability was effectively smoothed in the forecasted rainfall, which had much lower interannual variability (Figure 6). Despite this, the total forecasted wet season rainfall (about 40 inches for both the RCP4.5 and RCP8.5 scenarios) was higher than the observed wet season rainfall by 19%. Furthermore, the total dry season rainfall (for both the RCP4.5 and RCP8.5 scenarios) was forecasted to increase by 11% compared to the observed dry season rainfall. Overall, the forecasted rainfall will have a large number of rainy days.

The observed total annual mean flow, from the representative Shark River Slough station S333, of around 5.2 billion gallons per year is expected to increase to around 5.6 billion gallons per year. This 5% flow increase is potentially driven by forecasted increases in rainfall that would cause dry season water levels and flows in the Everglades to increase.

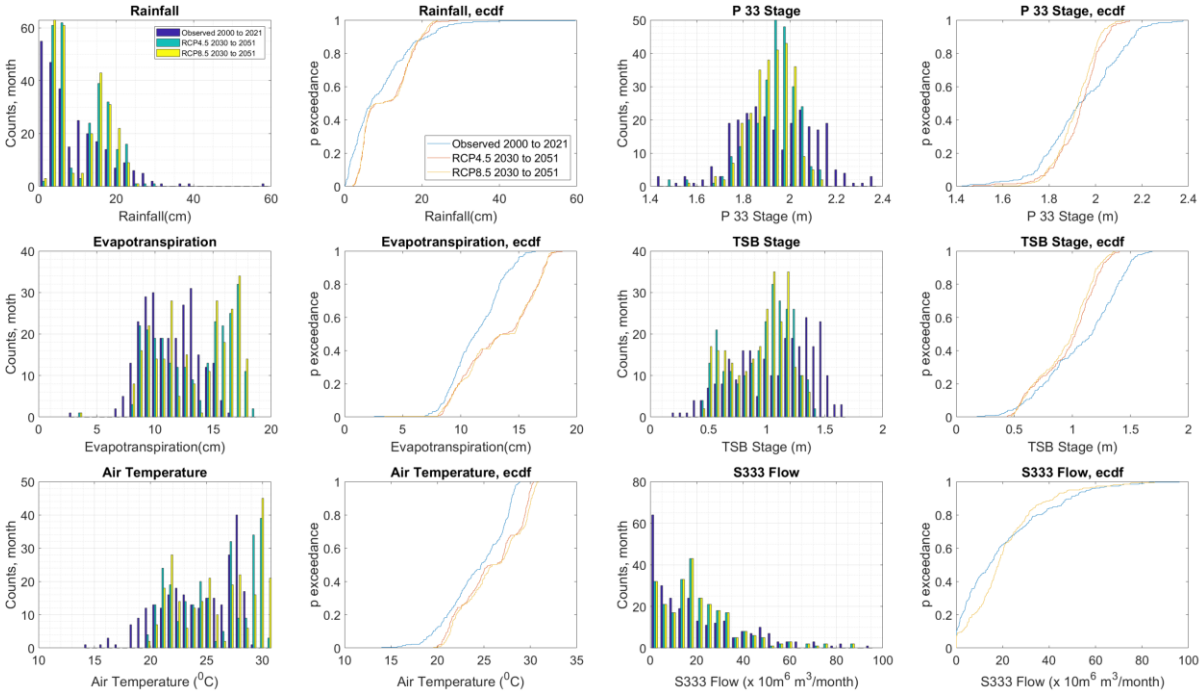

Figure 6. Histograms and empirical cumulative frequency distribution functions of observed and forecasted data sets evaluated based on the monthly aggregated datasets. The observed datasets were used to develop the baseline ANN model, and the forecasted datasets were used to forecast the salinity using the model developed by the observed dataset.

Besides altering the flow regime in the Everglades and into the bay, an increased difference between rainfall and evaporation loss is another impact of climate change on the local salinity regime. ETP is predicted to have slightly greater increases than rainfall under climate change, leading to a hydrological deficit. Below average wet season rainfall (44.5 inches) with an increase in evaporation losses will result in a proportional increase in salinity. Furthermore, the wet season water levels in both the P33 and TSB stations are forecasted to be lower than the historical record but higher in the dry season. As indicated by the empirical cumulative frequency distribution function, the forecasted hydrological data showed fewer stage values that were very low during the dry season or very high during the wet season compared to the observed data. The altered freshwater runoff, precipitation, ETP, and sea level would impact salinity levels in Florida Bay. Restoration efforts would also increase freshwater flows into the Everglades and ultimately the bay. Because this work focuses on the ANN model and its application, we did not go into detail on the climate change forecasted data and hydrological modeling outputs.

3.2. Salinity in Florida Bay

The observed salinities exhibited characteristic differences with distance from the shore. Nearshore sites had a wider range in their salinities, reflecting their proximity to inflow sources, compared with further offshore sites. Salinities varied from near zero to 54.5 PSU and 66.2 PSU for Terrapin Bay and Garfield Bight, respectively (Figure 7). The nearshore sites had an overall mean of 31 PSU and a high coefficient of variation (around 30% and 40% variability for Garfield Bight and Terrapin Bay respectively). As illustrated by their high coefficients of variation, the nearshore site salinity records varied from hypersaline to freshwater (Figure 7). The offshore sites had an overall mean of 36 PSU with coefficients of variation ranging from 10% to 15%.

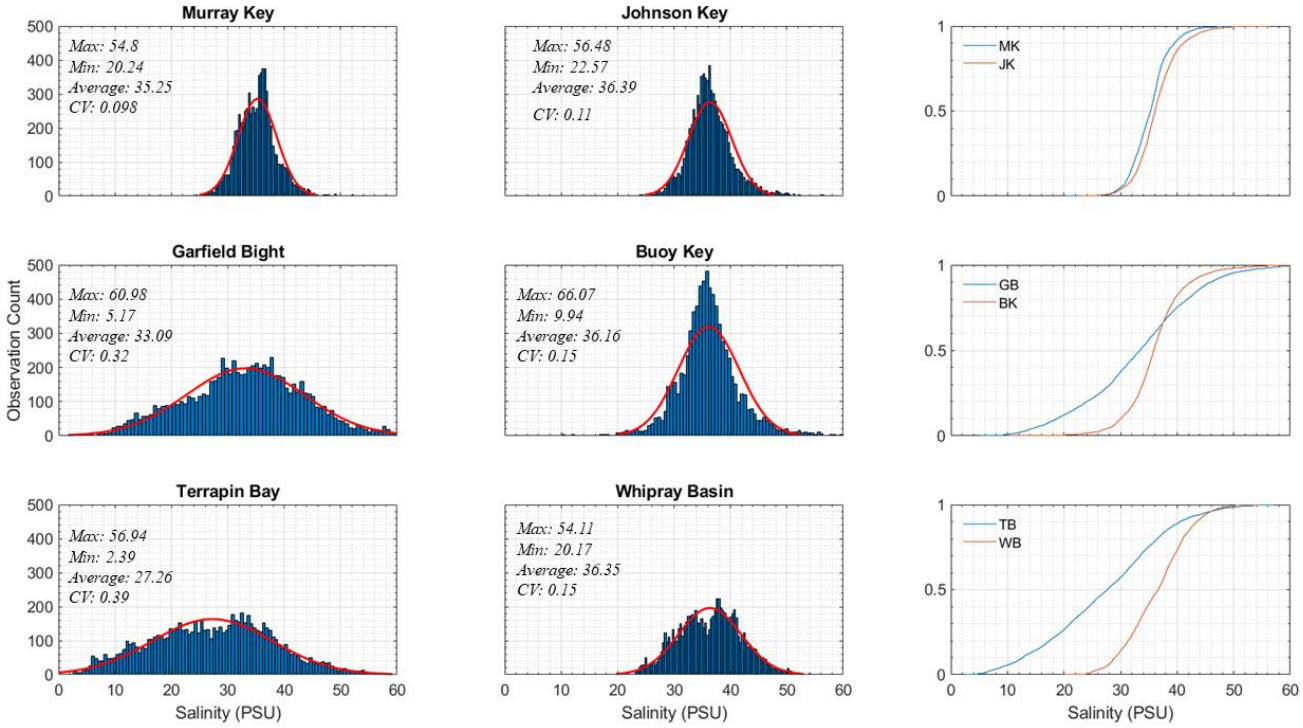

Figure 7. Histograms of observed salinities for both nearshore (**first panel**) and offshore sites (**second panel**) and their respective empirical cumulative distribution functions (**third panel**). Red lines show the normal distributions for the salinities.

Nearshore hypersaline conditions in Florida Bay have been previously reported [18,75]; these conditions were observed in the dry season when ETP was higher than rainfall. We found that Florida Bay was in hydrological deficit, as more than 75% of the time ETP was greater than the rainfall. In addition, the recurrence of hypersaline conditions followed a seasonal pattern. Beside rainfall and ETP, freshwater input into the bay varied seasonally. Across all sites, the mean monthly salinities were the highest between April and June, reaching a maximum in May. During these dry periods, a positive freshwater balance in Florida Bay was maintained only if the volume of freshwater inflow from Shark River Slough and Taylor Slough exceeded the ETP loss.

3.3. Coastal Salinity Index

The coastal salinity index for the observed salinities illustrated when each site entered periods of relative coastal drought or coastal freshwater conditions (Figure 8). Overall, the sites spent 46% to 61% of 2000 to 2021 period in relative drought conditions. The nearshore areas spent a slightly higher amount of time in relative drought conditions (54%) versus the offshore region (50%). The maximum number of months spent in continuous relative drought conditions varied from 13 to 25 months in the sites. The nearshore sites' maximum number of months spent in continuous drought conditions was higher (mean of 21.3 months) versus the offshore sites' (mean of 16.7 months). For the nearshore sites, the maximum number of months spent in continuous drought conditions was 14 months for Murray Key, and 25 months for both Terrapin Bay and Garfield Bight. For the offshore sites, the maximum number of months spent in continuous drought conditions was 13 months for Johnson Key, 18 months for Buoy Key, and 19 months for Whipray Basin.

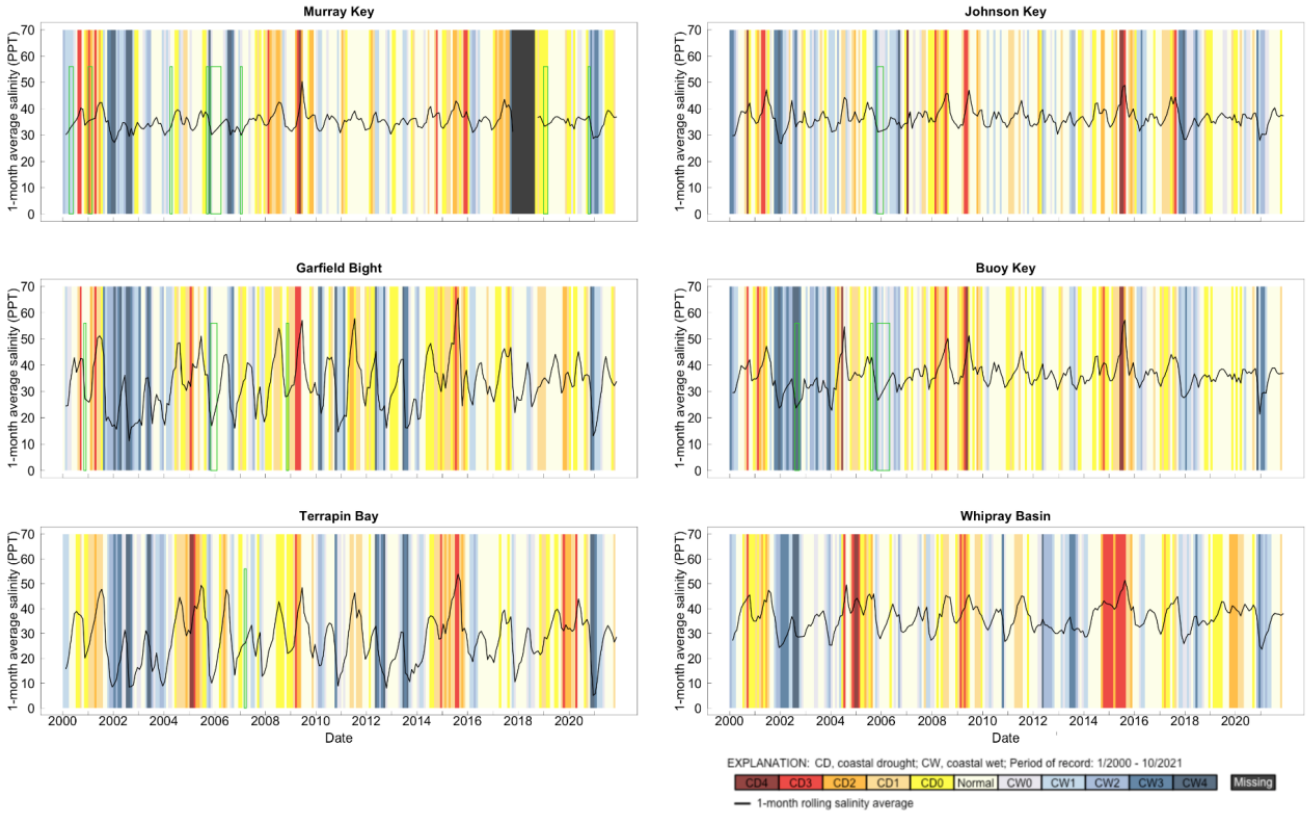

Figure 8. Coastal salinity index plots for observed salinity in all sites: Murray Key, Johnson Key, Garfield Bight, Buoy Key, Terrapin Bay, and Whipray Basin. The black line shows the mean monthly salinities while the colors represent either coastal drought classes (CD0 to CD4; yellow to red colors), normal salinity conditions (off white), or coastal freshwater classes (CW0 to CW4; gray to blue colors). The index represents changes in monthly salinity conditions with respect to average conditions in a site.

3.4. Artificial Neural Network Modeling

We developed one ANN model for each site (Murray Key, Johnson Key, Garfield Bight, Buoy Key, Terrapin Bay, and Whipray Basin) with acceptable objective function values (Figure 9 and Table S2) based on observed salinities for the study period (2000 to 2021). Our models were based on input variables representing the local hydrology, and atmospheric and tidal variables on a daily time scale for the 2000 to 2021 period. These variables included freshwater inflows, freshwater levels, air temperature, rainfall, evaporation, and a low pass filter of mean sea level rise. Our models were based on more than 7000 data points for all the variables.

We followed three model performance evaluations, based on model prediction (using two thirds of the input dataset), validation (based on one third of datasets) and combined performance (using the full dataset). The model performance during training and validation is given in the supplementary material Table S2, while the overall model performance is given below (Figure 9). The overall performance for each of the models had R^2 values of 0.79 or above. Compared to multiple linear regressions estimating salinity in Florida Bay, our models for these sites either had comparable or higher R^2 values [30], and our models had lower mean square errors compared to this previous work.

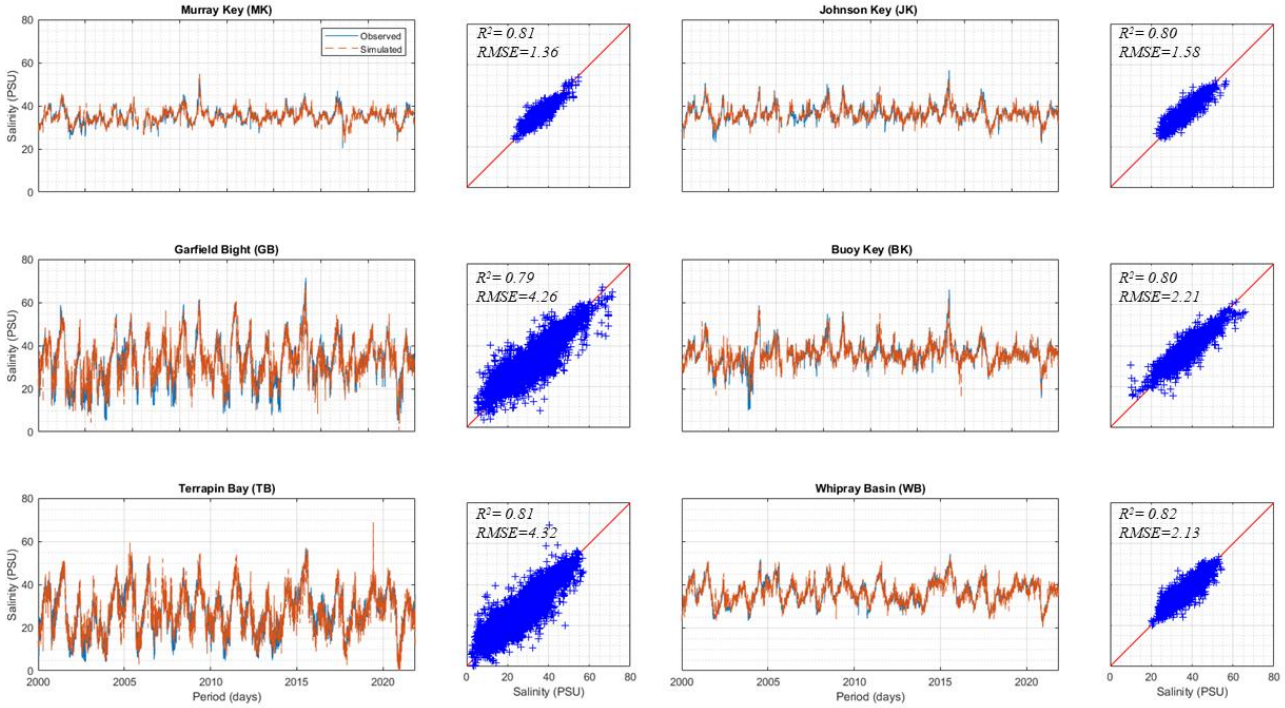

Figure 9. A sequential time series plot of observed and simulated salinities in each site, scatter plots of the observed and simulated salinities for each of the sites, and model performance measures.

The models for offshore salinities had higher levels of stability (RMSE of less than 2.5 PSU) while the nearshore sites were more dispersed around the mean with RMSE below 4.5 PSU. In all cases, the residuals were found to have an acceptable distribution. The models in the offshore sites showed greater stability than the nearshore sites. The nearshore sites, Garfield Bight and Terrapin Bay, exhibited salinities that ranged from near oligohaline to hypersaline conditions. Although this was well captured in our models, there was a larger error (4.3 PSU) in the model results for these sites as compared to others.

The plot of the observed data shows spikes or dips in salinity, which were mostly observed in all the sites. However, the nearshore sites had consistent wide-ranging fluctuations such as spikes in salinity that occurred in late 2004 and early 2015, or dips to freshwater levels in mid-2021. The observed salinity spikes in 2004 to 2007 were mostly consistent with the lower rainfall observed in 2004 and 2015 that also caused lower freshwater inflows and high evaporation losses in the bay. Overall drought conditions, in particular dry season dryness, has been highly correlated with the incidence of hypersaline conditions in the bay.

3.5. Impact of Climate Change on Salinities in Florida Bay

For most sites, mean daily salinities increased from the observed conditions to the RCP4.5 scenario, and increased again from the RCP4.5 to RCP8.5 scenarios. An ANOVA revealed significant differences between the three scenarios for all sites. A post hoc Tukey test using a Bonferroni correction revealed that salinity level varied significantly among all three scenarios for Garfield Bight, Johnson Key, Terrapin Bay, and Whipray Basin (p-value < 0.0001; Table 2). For Buoy Key and Murray Key, salinities varied significantly between the observed data and the two climate change scenarios (p-value< 0.0001), but not between the two climate change scenarios (p-value > 0.13; Table 2).

Table 2. Mean daily salinities (PSU) for the baseline scenario, and the RCP4.5 and RCP8.5 climate change scenarios.

Site	Scenario	Mean	Min	Max	Range	Std Dev	Difference with Baseline	Difference with RCP4.5
Murray Key	Baseline	35.25	20.34	46.98	34.46	3.44	NA	NA
	RCP4.5 *	33.66	13.48	49.28	35.81	5.5	−1.59	NA
	RCP8.5 *	33.52	13.71	48.94	35.22	5.38	−1.74	−0.15
Johnson Key	Baseline	36.39	22.57	56.48	33.91	3.86	NA	NA
	RCP4.5 *	41.83	29.35	66.69	37.34	6.07	5.43	NA
	RCP8.5 *‡	42.35	26.71	66.09	39.38	5.91	5.95	0.52
Garfield Bight	Baseline	33.09	5.17	71.38	66.21	10.46	NA	NA
	RCP4.5 *	38.18	2.17	71.94	69.77	11.86	5.08	NA
	RCP8.5 *‡	39.82	2.88	71.01	68.12	11.9	6.73	1.65
Buoy Key	Baseline	36.16	9.94	66.07	56.13	5.44	NA	NA
	RCP4.5 *	35.13	7.91	67.67	59.77	8.12	−1.03	NA
	RCP8.5 *	34.92	7.16	61.29	54.13	7.69	−1.24	−0.21
Terrapin Bay	Baseline	27.26	2.29	56.94	54.54	10.62	NA	NA
	RCP4.5 *	36.22	6.24	69.41	63.17	11.77	8.97	NA
	RCP8.5 *‡	46.58	25.46	57.63	32.17	6.02	19.33	10.36
Whipray Basin	Baseline	36.35	20.17	54.11	33.94	5.54	NA	NA
	RCP4.5 *	45.7	23.62	65.98	8.68	6.55	9.35	NA
	RCP8.5 *‡	46.23	23.74	67.37	43.63	6.1	9.88	0.53

Notes: * Significantly different from baseline values, ‡ Significantly different from RCP4.5 scenario.

The forecasted salinity conditions indicated wide ranging fluctuations that changed rather quickly over a given year. However, the variability in salinity for both the nearshore and offshore sites are expected to evolve over time, but differently for each region. For the nearshore sites Garfield Bight and Terrapin Bay, the RCP4.5 and RCP8.5 scenarios showed a systemic shift of the mean, minimum, and maximum salinity values compared to the observed salinities (Figure 10). We observed that Terrapin Bay's mean observed salinity of 27.3 PSU was predicted to increase by over 33% and 71% under the RCP4.5 and RCP8.5 forecasts, respectively. Likewise, the mean observed salinity of 33.09 PSU at Garfield Bight is forecasted to increase by 15% and 20% under the RCP4.5 and RCP8.5 forecasts, respectively (Table 2). As such, the empirical cumulative distribution functions for the nearshore salinities were shifted to the right, indicating a low probability for freshwater conditions, and a higher probability of increased salinity. These forecasted salinity conditions under climate change demonstrate that the nearshore estuarine area will evolve from polyhaline (18 to 30 PSU) to euhaline (30 to 35 PSU) conditions. Furthermore, the RCP8.5 scenario presents the highest probability for the occurrence of extreme salinity conditions (metahaline 40 to 55 PSU) in the nearshore estuarine ecosystem. Both the RCP4.5 and RCP8.5 scenarios showed the potential of nearshore salinities oscillating between polyhaline (18 to 30 PSU) to euhaline (30 to 40 PSU) conditions, and frequently overshooting to metahaline conditions (40 to 55 PSU).

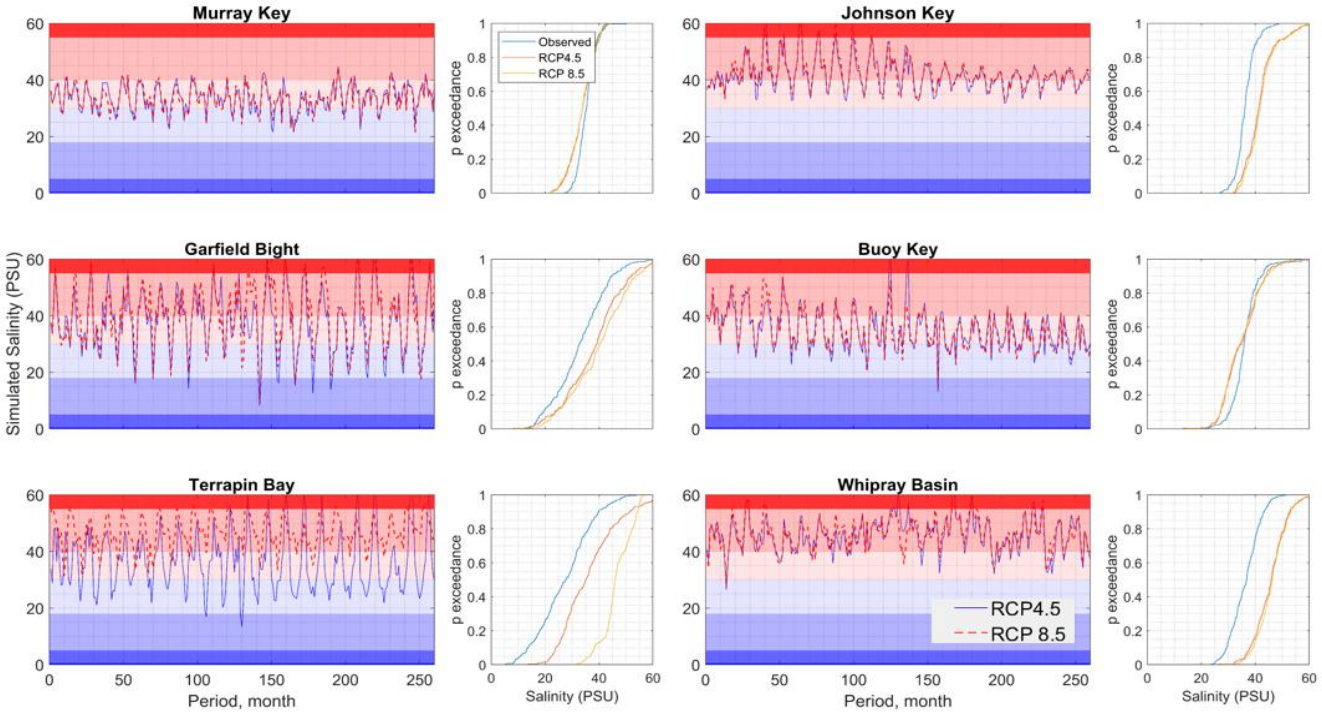

Figure 10. Forecasted salinities for the RCP4.5 and RCP8.5 scenarios and their empirical cumulative distribution functions (right of each sites' time series plot) comparing the climate change scenarios with observed salinities. The plots are based on monthly mean salinity values, and the background shades represent the following salinity classes: oligohaline (0.5 to 5 PSU) dark purple, mesohaline (5 to 18 PSU) medium purple, polyhaline (18 to 30 PSU) light purple, euhaline (30 to 40 PSU) light red, metahaline (40 to 55 PSU) medium red, and hypersaline (>55 PSU) dark red.

The mean offshore salinities were predicted to range from 34.92 to 46.23 PSU. Furthermore, the forecasted results suggested that the nearshore area would have metahaline (>45 PSU) conditions during short periods of time. With higher air temperatures and ETP under climate change, the possibility for nearshore salinities to drop into freshwater conditions was minimal. Although this line of analysis was based on the observations from both climate change scenarios, the empirical cumulative distribution functions for the RCP8.5 scenario were slightly shifted to the right of the RCP4.5 scenario (Figure 10), indicating the RCP8.5 scenario had a potential for higher salinity conditions.

When looking at the temporal evolution of the salinity regime, for both the RCP4.5 and RCP8.5 climate change scenarios; the offshore sites showed a wide range of salinity fluctuations (generally from polyhaline and euhaline to hypersaline; Figure 10) in earlier stages of the simulation. In the latter stages, the salinity regimes in the offshore sites exhibited decreasing fluctuations. As climate change effects persisted, particularly the effects of sea level rise and increased ETP, the forecasted model indicated that salinity in the offshore region of the bay would start to stabilize around the mean as shown in the Johnson Key plot (Figure 10). This phenomenon in the offshore region was associated with sea level rise that would cause increased marine conditions in that part of the bay. Unlike the offshore sites, the nearshore sites started with a smaller salinity range followed by gradually widening salinity ranges. This shift in the nearshore salinity range was controlled by the balance between freshwater input from inflow and rainfall as well as evaporative losses that caused a rapid shift in salinity regime and occurrence of extreme conditions.

The relative weights of the independent variables for predicting salinity (Table 3) indicated that forecasted salinities in the nearshore Terrapin Bay and Garfield Bight sites were mostly determined by the water levels in Taylor Slough (30% to 40% weight). A visible discrepancy existed between the forecasted salinity between the RCP4.5 and RCP8.5

scenarios in Terrapin Bay, since it is located at the mouth of Taylor River and small changes in the freshwater head affected this nearshore area the most. In fact, the water levels in Taylor Slough are highly correlated with freshwater inflow from Taylor Slough and Shark River Slough into the bay. Moving further away from the shoreline, salinity changes were increasingly controlled by sea level rise, and the importance of rainfall, water level and freshwater stages in the Everglades decreased.

Table 3. Range of input variables' weights for forecasting salinities under the RCP4.5 and RCP8.5 climate change scenarios. The input variables' weights were calculated using the random forest classification algorithm. Color codes show the weights of the variables for each site; blue refers to relatively higher weights, white refers to intermediate weights, and red refers to lower weights.

Input Variables	Murray Key	Johnson Key	Garfield Bight	Buoy Key	Terrapin Bay	Whipray Basin
Mean Sea Level	8–12	18–21	6–7	23–35	7–8	14–21
Rainfall	13–15	2–3	2–3	8–9	9–12	3–5
ETP	6–7	20–24	19–22	7–9	7–9	6–7
Air Temp	19–27	5–6	5–6	10–11	13–23	15–16
Shark River Slough Stage	7–8	20–26	22–23	9–19	11–15	25–33
Shark River Slough Flow	19–23	4–5	8–10	12–13	4–6	13–14
Taylor Slough Stage	17–18	22–24	30–34	17–18	34–43	13–14

3.6. Coastal Salinity Index for Salinities under Climate Change

The coastal salinity index for the predicted salinities under the RCP4.5 scenario illustrated when each site entered periods of relative coastal drought or coastal freshwater conditions (Figure 11). Overall, the sites spent 46% to 55% of 2030 to 2051 period in relative drought conditions. Both the nearshore and offshore sites spent 51% of the time in relative drought conditions. The maximum number of months spent in relative continuous drought conditions varied from 7 to 23 months in the sites. The nearshore sites' maximum number of months spent in continuous drought conditions was lower (mean of 9 months) versus the offshore sites (mean of 14.7 months). For the nearshore sites, the maximum number of months spent in continuous drought conditions was 11 for Murray Key, and 7 months for Terrapin Bay, and 9 months for Garfield Bight. For the offshore sites, the maximum number of months spent in continuous drought conditions was 11 for Johnson Key, 10 months for Buoy Key, and 23 months for Whipray Basin.

Under the RCP8.5 scenario, the sites spent 46% to 54% of 2030 to 2051 period in relative drought conditions (Figure 11). The nearshore and offshore sites experienced relative drought 51% and 48% of the time, respectively. The maximum number of months spent in relative continuous drought conditions varied from 9 to 15 months in the sites. The nearshore sites' maximum number of months spent in continuous drought conditions was lower (mean of 11.3 months) versus the offshore sites' (mean of 13.3 months). For the nearshore sites, the maximum number of months spent in continuous drought conditions was 9 for Murray Key, 15 months for Terrapin Bay, and 10 months for Garfield Bight. For the offshore sites, the maximum number of months spent in continuous drought conditions was 12 for Johnson Key, 18 months for Buoy Key, and 10 months for Whipray Basin.

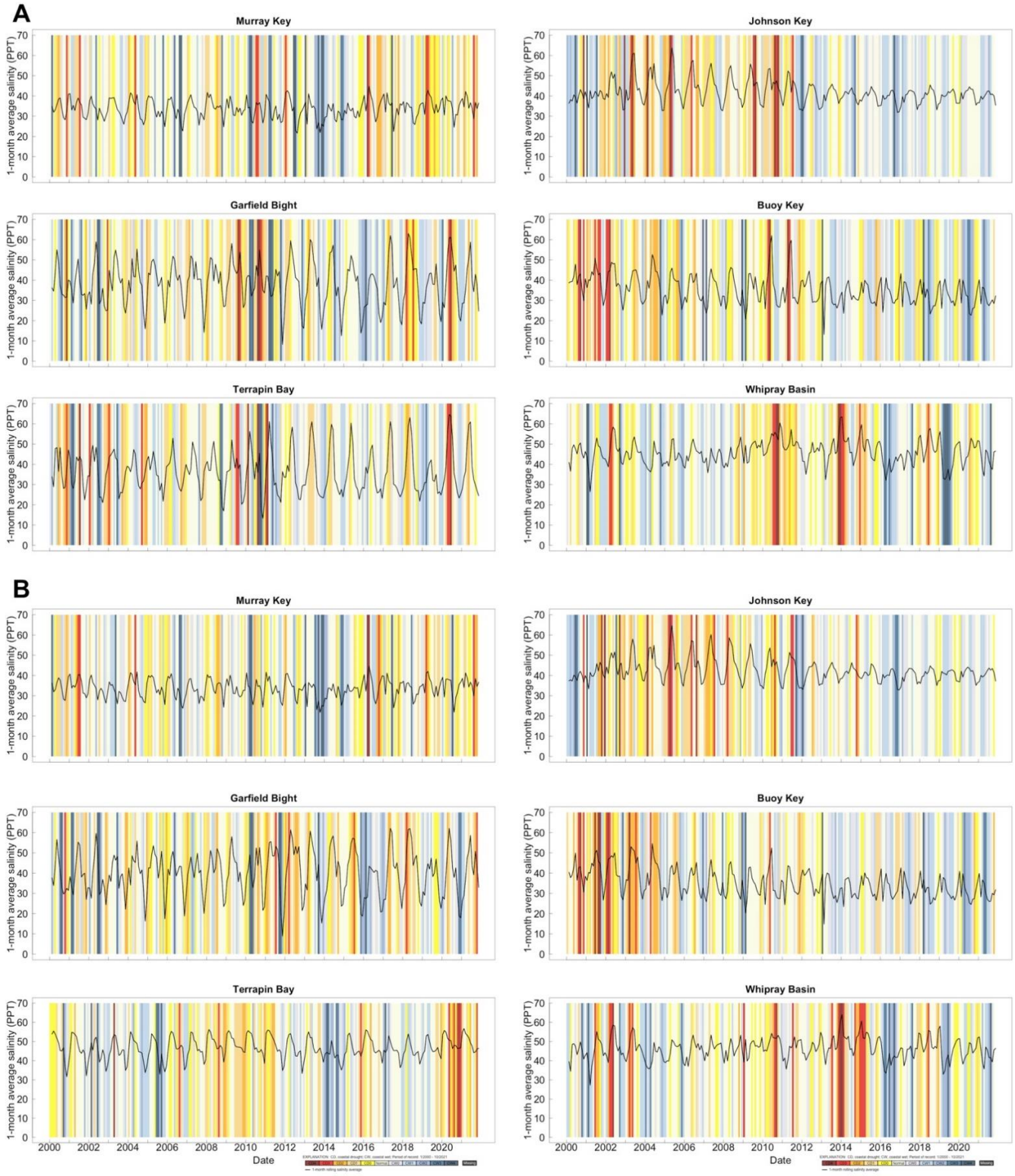

Figure 11. Coastal salinity index plots for predicted salinities in the RCP4.5 scenario (**A**) and RCP8.5 scenario (**B**) for all sites: Murray Key, Johnson Key, Garfield Bight, Buoy Key, Terrapin Bay, and Whipray Basin. The black line shows the mean monthly salinities while the colors represent either coastal drought classes (CD0 to CD4; yellow to red colors), normal salinity conditions (off white), or coastal freshwater classes (CW0 to CW4; gray to blue colors). The index represents changes in monthly salinity conditions with respect to average conditions in a site.

4. Discussion

We found ANN modeling to be a robust and replicable tool for predicting salinity in Florida Bay and understanding the impacts of climate change. With the emergence of high-performance computing technology and skill sets, artificial intelligence and machine learning are increasingly used in various fields of study. In addition to FF-ANN, gene-expression programming, evolutionary polynomial regressions, model trees, and support vector machine models are widely used in various water resources and environmental studies [62]. Among others, deep neural network modeling approaches, such as the FF-ANN, are acknowledged for their strength in evaluating environmental systems, and forecasting and analyzing systems sensitive to changes in environmental variables. ANN models have been effectively developed for rainfall runoff, and forecasting water quality and water demand systems. The American Society of Civil Engineers has identified ANN modeling as an emerging tool for hydrological modeling [35,36]. Such tools are valuable for planning and decision making in a managed hydrologic regime that is also highly susceptible to climate change.

Based on the neural network forecast and coastal salinity index analysis results, we demonstrated that the effect of climate change in estuaries varied in space and time in this study. Nearshore estuarine regions were subject to an increasing range of salinity characterized by frequent extreme conditions. In order to maintain the nearshore estuarine ecosystem and its ecosystem services, adequate freshwater supply is important, particularly in the dry season. Likewise, monitoring and potentially controlling the presence of rapid changes in the salinity regime of nearshore regions under climate change is critical. Offshore regions were affected by climate change quite differently from that of nearshore regions. In these regions, the salinity range was predicted to behave much like the nearshore regions for some time. However, as sea level rise persists, the salinity fluctuations were predicted to dampen and settle close to mean oceanic salinity levels.

Climate change impacts to local hydrological factors and sea level rise are likely to change salinity regimes in Florida Bay. Projected changes in rainfall and higher ETP were the key variables that influenced freshwater stages in the Everglades, which played a principal role in regulating salinity changes from 2030 to 2051 in both nearshore and offshore regions. While these sites regularly experience salinity fluctuations following seasonal hydrological patterns for the area, dry season salinities in both nearshore and offshore regions of the bay are usually high. Furthermore, under climate change, those dry season salinities are forecasted to reach hypersaline conditions. The nearshore region exhibited more volatility in salinity than the offshore region in the bay, due to proximity to freshwater inflow sources in the wet season and reduced connection with tidal flushing during the dry season. During the wet season, the salinity regime in the nearshore enters a mesohaline (5 to 18 PSU) to polyhaline (18 to 30 PSU) range, while the offshore sites remain within a polyhaline (18 to 30 PSU) to euhaline (30 to 40 PSU) range. As sea levels continue to rise, two distinct outcomes may occur. First, salinities in the nearshore region of the bay may experience extremes, fluctuating between fresh to hypersaline conditions. According to our modeling results, both freshwater inflow and sea level rise will be the primary drivers behind these large oscillations in salinity conditions in the nearshore area. However, the offshore region is predicted to evolve from varying between polyhaline and euhaline ranges to hypersaline conditions into marine conditions (euhaline to metahaline ranges) with a decreased range of salinity (Figure 10).

Historically, freshwater flows from the Everglades maintained brackish conditions (<30 PSU) in many basins in the bay [76]. Compared to these historic, pre-drainage conditions, Florida Bay currently receives 2.5 to 4 times less freshwater [12,76,77]. Consequently, salinity has increased from 5.3 to 20.1 PSU on average in the bay compared to pre-drainage conditions, with the largest differences occurring in areas where freshwater enters the bay [76].

To preserve the current estuarine system in the nearshore areas, freshwater management will be necessary for Florida Bay, and continued efforts to provide sufficient flows

of freshwater will be vital. These flows will help control salinity spikes during low flow conditions. Particularly during the dry season, the system suffers from a hydrological deficit from high evaporative losses. Under climate change, the effect of dry season evaporation will be much greater and will be particularly acute for the nearshore salinity regime, which can spike to hypersaline conditions. The optimum freshwater inflow volume, or the freshwater levels in both Shark River Slough and Taylor Slough, did not occur every day. However, in this study we found that both the wet season and dry season freshwater inflow into the bay directly impacted the nearshore salinity of the bay. Because dry season rainfall in the bay is quite limited, the salinity in the bay is predominantly driven by extreme evaporation conditions. In the absence of freshwater inflow, dry season salinity would remain hypersaline for weeks and even months, creating unfavorable conditions for the flora and fauna in the area [78].

These predicted future increases and potential rapid fluctuations in salinity will present unfavorable conditions for the species that flourish in a transitional and more stable estuarine environment. Recent increases in bay salinity have had negative impacts on numerous animals in the bay including red drum, common snook, American crocodiles, roseate spoonbills, mangrove terrapins, ospreys, West Indian manatees, and bottlenose dolphins [78]. The optimal habitat for spotted seatrout is predicted to decrease with salinity increases, while habitat for spiny lobster may increase with rising salinities [32]. Decreases in freshwater flows to Florida Bay led to changes in the composition of seagrass communities, which may have been associated with declines in game fish populations [29,79]. Higher salinities under climate change could potentially increase the risk of seagrass die-offs, seagrass wasting disease, and algal blooms in the bay [21–23]. Our study sites were also within the epicenter of two major seagrass die-off events in the late 1980s and 2015 [19,20]. A continued and sustainable dry season freshwater supply would help maintain suitable estuarine conditions for the ecosystem of Florida Bay.

The generalizations of this study are limited by the uncertainty of the climate downscaled data and its application to a forecasted hydrological model with a large grid size (2 miles by 2 miles). Our study included the impacts of sea level rise but did not consider changes in landscape features, connectivity, residence times in the basins, or circulation patterns in the bay. We also did not account for the effects of wind on salinity since those input factors did not substantially improve model performance. While our approach can be considered an oversimplification since it ignored these factors, it demonstrated that neural network models can be used to provide scientific evidence for water management and flow regulation decisions.

Implications for Sustainable Management of Estuaries

Estuarine ecosystems are greatly vulnerable to the adverse effects of climate change. Among others, changes in freshwater inflow, increasing water temperature, evaporation, and sea level rise are the primary challenges that estuaries face. For instance, sea level rise, decreasing freshwater inflow, and other factors have destroyed much estuarine habitat in the western USA [9]. Furthermore, estuaries are likely to experience changes in factors besides salinity including dissolved oxygen, water temperatures, suspended sediments, pH, wind stress, and nutrient concentrations under climate change [3]. Unfortunately, estuaries are among the most threatened ecosystems worldwide [80]. Yet, they are critical habitat for fisheries and nurseries, while providing filtering and detoxification services and opportunities for recreation and tourism [3,80]. Tools to help understand the key drivers of change and their magnitude affecting the health and sustainability of estuaries are important to design adaptive strategies for these challenges.

In this study, we illustrated a reliable technique to identify input parameters for ANN salinity forecast modeling under climate change. While the ANN's generic mathematical formulation is entirely data driven, in our study, we used a combination of hydrological, atmospheric and statistics as key selection criteria. Our study demonstrated the benefits of artificial intelligence and machine learning techniques in modeling the hydrological

complexity in estuarine systems. It also provided meaningful results while avoiding the computational limitations of other hydrodynamic modeling protocols.

5. Conclusions

Providing more freshwater flow into Florida Bay to mitigate high-salinity events, minimize risk of seagrass die-offs, and improve the ecological health of the bay is a main goal of the Comprehensive Everglades Restoration Plan (CERP). Several components of CERP, including the Central Everglades Project, a reservoir in the Everglades Agricultural Area, and C-111 Spreader Canal Western Project should increase freshwater flows through Shark River Slough and Taylor Slough into Florida Bay [81]. CERP has been shown in other modeling work to lower salinities in Florida Bay, with the largest benefit in the central region of the bay [82]. Increased freshwater flow would also provide a freshwater head to delay the movement of saltwater inland and offset sea level rise. Given the potential impacts of climate change on Florida Bay, restoration efforts should be expedited to maintain healthy, estuarine conditions in this ecosystem.

Our model can be used for salinity forecasting under climate change while the input variables are available. Other salinity regression modeling work in Florida Bay and other Everglades estuaries found the strongest correlative relationships between salinity and freshwater stage in the Everglades, followed by sea level and wind parameters [30]. Similarly, our random forest classification algorithm results for the climate change scenarios showed that, for most sites, Everglades stage levels (in Shark River Slough and Taylor Slough) had the highest relative weights in predicting salinity (Table 3). While we excluded wind parameters from our analysis, we also had strong relative weights for sea level in the offshore sites under climate change (Table 3).

We could expect greater impacts to many species under RCP8.5 due to its relatively higher predicted salinity versus RCP4.5. It is also important to note that species in Florida Bay may face multiple stressors in addition to higher salinities under climate change such as increases in temperature, reductions in prey availability, ocean acidification, decreases in dissolved oxygen, sea level rise, increased spread of invasive species, and increases in CO_2 [8,8,78,83–88]. The predicted drier conditions and changes in salinity under climate change emphasize the need for restored freshwater flows into the bay.

Supplementary Materials: The following supporting information can be downloaded at: https://www.mdpi.com/article/10.3390/w14213495/s1, Our manuscript includes two tables with model performance metrics and coastal salinity index values and two figures with annual tidal fluctuations and regression equations for the observed and forecasted sea levels. Table S1: Classifications for Coastal Salinity Index values; Table S2: Model performance evaluation for training and validation stages for every site; Figure S1. Annual observed sea level data (A), Annual forecasted sea level data (B), Low pass, smoothed observed sea level data (C), Low pass, smoothed forecasted sea level data; Figure S2. Observed and forecasted sea level with the regression trend line (dashed purple line), mean water levels (light blue line), regression equations, and R-squared values

Author Contributions: Conceptualization, A.Z.A., R.P.W. and S.E.D.; Methodology, A.Z.A., R.P.W. and S.E.D.; Validation, A.Z.A., R.P.W. and S.E.D.; Formal Analysis, A.Z.A. and R.P.W.; Investigation, A.Z.A. and R.P.W.; Resources, A.Z.A., R.P.W. and S.E.D.; Data Curation, A.Z.A. and R.P.W.; Writing—Original Draft Preparation, A.Z.A. and R.P.W.; Writing—Review and Editing, A.Z.A., R.P.W., G.L.L., A.M.M. and S.E.D.; Visualization, A.Z.A. and R.P.W.; Supervision, A.M.M. and S.E.D.; Project Administration, A.Z.A., R.P.W. and S.E.D.; Funding Acquisition, A.Z.A., R.P.W. and S.E.D. All authors have read and agreed to the published version of the manuscript.

Funding: This study was supported by The Everglades Foundation.

Institutional Review Board Statement: Not applicable.

Informed Consent Statement: Not applicable.

Data Availability Statement: We used data from the South Florida Water Management District's (SFWMD) environmental database, DBHydro (https://www.sfwmd.gov/science-data/dbhydro (accessed on 10 December 2021)) for the following daily mean salinity (PSU), daily mean stage (feet), daily mean flow (cubic feet per second), daily total rainfall (inches), daily mean potential evapotranspiration (ETP, inches), and daily mean air temperatures (°C). Daily mean sea level at Vaca Key was obtained from the National Oceanic and Atmospheric Administration's Tides and Currents database (https://tidesandcurrents.noaa.gov/map/index.html?region=Florida (accessed on 10 December 2021)). We used localized constructed analogs (LOCA) downscaled data (Pierce et al. 2014) from 27 Global Circulation Models that were available daily and in 1/16th degree grid resolution. These datasets can be downloaded publicly from Lawrence Livermore National Laboratory (https://gdo-dcp.ucllnl.org/downscaled_cmip_projections/dcpInterface.html (accessed on 10 December 2021)). We used the Coordinated Regional Climate Downscaling Experiment (CORDEX) initiative (https://cordex.org/data-access/how-to-access-the-data/ (accessed on 10 December 2019)) for additional future projected data required to estimate ETP.

Acknowledgments: Any opinions, findings, conclusions, or recommendations expressed in the material are those of the authors and do not necessarily reflect the views of The Everglades Foundation. We acknowledge our data sources and extend our gratitude to the reviewers whose comments were helpful to improve the manuscript.

Conflicts of Interest: The authors declare no conflict of interest.

References

1. Kennish, M.J. Environmental Threats and Environmental Future of Estuaries. *Environ. Conserv.* **2002**, *29*, 78–107. [CrossRef]
2. Waycott, M.; Duarte, C.M.; Carruthers, T.J.; Orth, R.J.; Dennison, W.C.; Olyarnik, S.; Calladine, A.; Fourqurean, J.W.; Heck, K.L.; Hughes, A.R. Accelerating Loss of Seagrasses across the Globe Threatens Coastal Ecosystems. *Proc. Natl. Acad. Sci. USA* **2009**, *106*, 12377–12381. [CrossRef]
3. Gillanders, B.M.; Elsdon, T.S.; Halliday, I.A.; Jenkins, G.P.; Robins, J.B.; Valesini, F.J. Potential Effects of Climate Change on Australian Estuaries and Fish Utilising Estuaries: A Review. *Mar. Freshw. Res.* **2011**, *62*, 1115–1131. [CrossRef]
4. Duarte, C.M.; Borja, A.; Carstensen, J.; Elliott, M.; Krause-Jensen, D.; Marbà, N. Paradigms in the Recovery of Estuarine and Coastal Ecosystems. *Estuaries Coasts* **2015**, *38*, 1202–1212. [CrossRef]
5. Barbier, E.B. Marine Ecosystem Services. *Curr. Biol.* **2017**, *27*, R507–R510. [CrossRef] [PubMed]
6. Leal Filho, W.; Nagy, G.J.; Martinho, F.; Saroar, M.; Erache, M.G.; Primo, A.L.; Pardal, M.A.; Li, C. Influences of Climate Change and Variability on Estuarine Ecosystems: An Impact Study in Selected European, South American and Asian Countries. *Int. J. Environ. Res. Public Health* **2022**, *19*, 585. [CrossRef] [PubMed]
7. Orlando, S.P. *Salinity Characteristics of Gulf of Mexico Estuaries*; Strategic Environmental Assessments Division, Office of Ocean Resources Conservation and Assessment, National Ocean Service, National Oceanic and Atmospheric Administration: Silver Spring, MD, USA, 1993.
8. Rudnick, D.T.; Ortner, P.B.; Browder, J.A.; Davis, S.M. A Conceptual Ecological Model of Florida Bay. *Wetlands* **2005**, *25*, 870–883. [CrossRef]
9. Brophy, L.S.; Greene, C.M.; Hare, V.C.; Holycross, B.; Lanier, A.; Heady, W.N.; O'Connor, K.; Imaki, H.; Haddad, T.; Dana, R. Insights into Estuary Habitat Loss in the Western United States Using a New Method for Mapping Maximum Extent of Tidal Wetlands. *PLoS ONE* **2019**, *14*, e0218558. [CrossRef]
10. Martínez, M.L.; Costanza, R.; Perez-Maqueo, O. Ecosystem Services Provided by Estuarine and Coastal Ecosystems: Storm Protection as a Service from Estuarine and Coastal Ecosystems. In *Treatise on Estuarine and Coastal Science*; Academic Press: Cambridge, MA, USA, 2011; ISBN 0-12-374711-2.
11. UNESCO. *Operational Guidelines for the Implementation of the World Heritage Convention*; UNESCO World Heritage Center: Paris, France, 2015.
12. Smith, T.J., III; Hudson, H.J.; Robblee, M.B.; Powell, G.N.; Isdale, P.J. Freshwater Flow from the Everglades to Florida Bay: A Historical Reconstruction Based on Fluorescent Banding in the Coral Solenastrea Bournoni. *Bull. Mar. Sci.* **1989**, *44*, 274–282.
13. Marshall, F.; Brewster-Wingard, G.L. *Florida Bay Salinity and Everglades Wetlands Hydrology circa 1900 CE: A Compilation of Paleoecology-Based Statistical Modeling Analyses*; US Department of the Interior, US Geological Survey: Reston, VA, USA, 2012.
14. McIvor, C.C.; Ley, J.A.; Bjork, R.D. Changes in Freshwater Inflow from the Everglades to Florida Bay Including Effects on Biota and Biotic Processes: A Review. In *Everglades: The Ecosystem and Its Restoration*; Routledge Taylor & Francis Group: Abingdon, UK, 1994; pp. 117–146.
15. Marshall, F.; Smith, D.; Nuttle, W. Simulating and Forecasting Salinity in Florida Bay: A Review of Model; Critical Ecosystem Studies Initiative Final Project Report. 2008. Available online: https://scholar.google.co.uk/scholar?hl=en&as_sdt=0%2C5&q=Simulating+and+Forecasting+Salinity+in+Florida+Bay%3A+A+Review+of+Model&btnG= (accessed on 10 December 2021).
16. Kotun, K.; Renshaw, A. Taylor Slough Hydrology. *Wetlands* **2014**, *34*, 9–22. [CrossRef]

17. Wanless, H.R.; Tagett, M.G. Origin, Growth and Evolution of Carbonate Mudbanks in Florida Bay. *Bull. Mar. Sci.* **1989**, *44*, 454–489.
18. Nuttle, W.K.; Fourqurean, J.W.; Cosby, B.J.; Zieman, J.C.; Robblee, M.B. Influence of Net Freshwater Supply on Salinity in Florida Bay. *Water Resour. Res.* **2000**, *36*, 1805–1822. [CrossRef]
19. Robblee, M.B.; Barber, T.; Carlson, P., Jr.; Durako, M.; Fourqurean, J.W.; Muehlstein, L.; Porter, D.; Yarbro, L.; Zieman, R.; Zieman, J.C. Mass Mortality of the Tropical Seagrass Thalassia Testudinum in Florida Bay (USA). *Mar. Ecol. Prog. Ser.* **1991**, *71*, 297–299. [CrossRef]
20. Hall, M.O.; Furman, B.T.; Merello, M.; Durako, M.J. Recurrence of Thalassia Testudinum Seagrass Die-off in Florida Bay, USA: Initial Observations. *Mar. Ecol. Prog. Ser.* **2016**, *560*, 243–249. [CrossRef]
21. Blakesley, B.A.; Berns, D.M.; Hall, M.O. Infection, Infestation, and Disease: Differential Impacts of *Labyrinthula* Sp. on the Seagrass Thalassia Testudinum (Banks Ex König) in Florida Bay, USA. In *Proceedings of the Florida Bay Program & Abstracts, Joint Conference on the Science and Restoration of the Greater Everglades and Florida Bay Ecosystem*; University of Florida: Gainesville, FL, USA, 2003; pp. 135–137.
22. Fourqurean, J.W.; Robblee, M.B. Florida Bay: A History of Recent Ecological Changes. *Estuaries Coasts* **1999**, *22*, 345–357. [CrossRef]
23. Butler IV, M.J.; Hunt, J.H.; Herrnkind, W.F.; Childress, M.J.; Bertelsen, R.; Sharp, W.; Matthews, T.; Field, J.M.; Marshall, H.G. Cascading Disturbances in Florida Bay, USA: Cyanobacteria Blooms, Sponge Mortality, and Implications for Juvenile Spiny Lobsters Panulirus Argus. *Mar. Ecol. Prog. Ser.* **1995**, *129*, 119–125. [CrossRef]
24. Swart, P.; Price, R. Origin of Salinity Variations in Florida Bay. *Limnol. Oceanogr.* **2002**, *47*, 1234–1241. [CrossRef]
25. Kelble, C.R.; Johns, E.M.; Nuttle, W.K.; Lee, T.N.; Smith, R.H.; Ortner, P.B. Salinity Patterns of Florida Bay. *Estuar. Coast. Shelf Sci.* **2007**, *71*, 318–334. [CrossRef]
26. CERP–SEPM. *System-Wide Performance Measure: Southern Estuaries Performance Measure–Salinity*; CERP: Lahore, Pakistan, 2008.
27. Southeast Florida Regional Climate Change Compact Sea Level Rise Work Group (Compact). *A Document Prepared for the Southeast Florida Regional Climate Change Compact Climate Leadership Committee*; Southeast Florida Regional Climate Change Compact Sea Level Rise Work Group (Compact): Miami, FL, USA, 2020; p. 36.
28. Cosby, B.J.; Marshall, F.E.; Nuttle, W.K. *FATHOM Model Structure and Salinity Simulation*; South Florida Water Management District: Palm Beach, FL, USA, 2010.
29. Herbert, D.A.; Perry, W.B.; Cosby, B.J.; Fourqurean, J.W. Projected Reorganization of Florida Bay Seagrass Communities in Response to the Increased Freshwater Inflow of Everglades Restoration. *Estuaries Coasts* **2011**, *34*, 973–992. [CrossRef]
30. Marshall, F.; Smith, D.; Nickerson, D. Empirical Tools for Simulating Salinity in the Estuaries in Everglades National Park, Florida. *Estuar. Coast. Shelf Sci.* **2011**, *95*, 377–387. [CrossRef]
31. Park, J.; Stabenau, E.; Kotun, K. Florida Bay Assessment Model: User Manual. In *South Florida Natural Resources Center, US Department of the Interior, Everglades National Park, Homestead, FL, Hydrologic Model Manual*; SFNRC: Homestead, FL, USA, 2016; pp. 7–27.
32. Kearney, K.A.; Butler, M.; Glazer, R.; Kelble, C.R.; Serafy, J.E.; Stabenau, E. Quantifying Florida Bay Habitat Suitability for Fishes and Invertebrates under Climate Change Scenarios. *Environ. Manag.* **2015**, *55*, 836–856. [CrossRef] [PubMed]
33. Aumen, N.; Berry, L.; Best, R.; Edwards, A.; Havens, K.; Obeysekera, J.; Rudnick, D.; Scerbo, M. *Predicting Ecological Changes in the Florida Everglades under a Future Climate Scenario*; US Geological Survey, Florida Sea Grant, Florida Atlantic University: Boca Raton, FL, USA, 2013; Available online: http://wwwcesfauedu/climate_change/ecology-february-2013/PECFEFCS_Reportpdf (accessed on 10 December 2021).
34. Bonafe, A.; Galeati, G.; Sforna, M. Neural Networks for Daily Mean Flow Forecasting. *WIT Trans. Ecol. Environ.* **1970**, *7*, 8.
35. ASCE. Task Committee on Application of Artificial Neural Networks in Hydrology Artificial Neural Networks in Hydrology II: Hydrologic Applications. *J. Hydrol. Eng.* **2000**, *5*, 124–137. [CrossRef]
36. ASCE. Task Committee on Application of Artificial Neural Networks in Hydrology Artificial Neural Networks in Hydrology I: Preliminary Concepts. *J. Hydrol. Eng.* **2000**, *5*, 115–123. [CrossRef]
37. Deng, T.; Chau, K.-W.; Duan, H.-F. Machine Learning Based Marine Water Quality Prediction for Coastal Hydro-Environment Management. *J. Environ. Manag.* **2021**, *284*, 112051. [CrossRef] [PubMed]
38. Ubah, J.; Orakwe, L.; Ogbu, K.; Awu, J.; Ahaneku, I.; Chukwuma, E. Forecasting Water Quality Parameters Using Artificial Neural Network for Irrigation Purposes. *Sci. Rep.* **2021**, *11*, 1–13. [CrossRef]
39. Wang, S.; Peng, H.; Liang, S. Prediction of Estuarine Water Quality Using Interpretable Machine Learning Approach. *J. Hydrol.* **2022**, *605*, 127320. [CrossRef]
40. Wu, J.; Wang, Z. A Hybrid Model for Water Quality Prediction Based on an Artificial Neural Network, Wavelet Transform, and Long Short-Term Memory. *Water* **2022**, *14*, 610. [CrossRef]
41. Van Vuuren, D.P.; Edmonds, J.; Kainuma, M.; Riahi, K.; Thomson, A.; Hibbard, K.; Hurtt, G.C.; Kram, T.; Krey, V.; Lamarque, J.-F. The Representative Concentration Pathways: An Overview. *Clim. Change* **2011**, *109*, 5–31. [CrossRef]
42. Jubb, I.; Canadell, P.; Dix, M. *Representative Concentration Pathways (RCPs)*; Australian Government, Department of the Environment: Canberra, Australia, 2013.
43. Schomer, N.S.; Drew, R.D. *An Ecological Characterization of the Lower Everglades, Florida Bay and the Florida Keys*; Bureau of Land Management; Fish and Wildlife Service: Washington, DC, USA, 1982.

44. Boyer, J.N.; Fourqurean, J.W.; Jones, R.D. Spatial Characterization of Water Quality in Florida Bay and Whitewater Bay by Multivariate Analyses: Zones of Similar Influence. *Estuaries* **1997**, *20*, 743–758. [CrossRef]
45. Abiy, A.Z.; Melesse, A.M.; Abtew, W.; Whitman, D. Rainfall Trend and Variability in Southeast Florida: Implications for Freshwater Availability in the Everglades. *PLoS ONE* **2019**, *14*, e0212008. [CrossRef] [PubMed]
46. Pierce, D.W.; Cayan, D.R.; Thrasher, B.L. Statistical Downscaling Using Localized Constructed Analogs (LOCA). *J. Hydrometeorol.* **2014**, *15*, 2558–2585. [CrossRef]
47. Obeysekera, J. Validating Climate Models for Computing Evapotranspiration in Hydrologic Studies: How Relevant Are Climate Model Simulations over Florida? *Reg. Environ. Change* **2013**, *13*, 81–90. [CrossRef]
48. Stefanova, L.; Sura, P.; Griffin, M.; Chan, S.; Misra, V. *Non-Gaussian Winter Daily Minimum and Maximum Temperatures in a Regional Climate Model: Downscaling of Reanalysis, Historical Simulations and Future Projections for the Southeast United States*; American Geophysical Union: Washington, DC, USA, 2011; Volume 2011, p. GC51D-1015.
49. Penman, H.L. Natural Evaporation from Open Water, Bare Soil and Grass. *Proc. R. Soc. Lond. Ser. A Math. Phys. Sci.* **1948**, *193*, 120–145.
50. Allen, R.G.; Pereira, L.S.; Raes, D.; Smith, M. *Crop Evapotranspiration-Guidelines for Computing Crop Water Requirements*; FAO Irrigation and Drainage Paper 56; FAO: Rome, Italy, 1998; Volume 300, p. *D0* 5109.
51. Price, R.M.; Nuttle, W.K.; Cosby, B.J.; Swart, P.K. Variation and Uncertainty in Evaporation from a Subtropical Estuary: Florida Bay. *Estuaries Coasts* **2007**, *30*, 497–506. [CrossRef]
52. Abtew, W.; Obeysekera, J.; Shih, G. Spatial Analysis for Monthly Rainfall in South Florida 1. *JAWRA J. Am. Water Resour. Assoc.* **1993**, *29*, 179–188. [CrossRef]
53. Sweet, W.V.; Kopp, R.E.; Weaver, C.P.; Obeysekera, J.; Horton, R.M.; Thieler, E.R.; Zervas, C. *Global and Regional Sea Level Rise Scenarios for the United States*; U.S. Department of Commerce: Silver Spring, MD, USA, 2017.
54. Parris, A.S.; Bromirski, P.; Burkett, V.; Cayan, D.R.; Culver, M.E.; Hall, J.; Horton, R.M.; Knuuti, K.; Moss, R.H.; Obeysekera, J. *Global Sea Level Rise Scenarios for the United States National Climate Assessment*; NOAA: Washington, DC, USA, 2012.
55. Paudel, R.; Van Lent, T.; Naja, G.M.; Khare, Y.; Wiederholt, R.; Davis, S.E., III. Assessing the Hydrologic Response of Key Restoration Components to Everglades Ecosystem. *J. Water Resour. Plan. Manag.* **2020**, *146*, 04020084. [CrossRef]
56. U.S. Army Corps of Engineers and South Florida Water Management District. *South Florida Water Management District. Central and Southern Florida Project Comprehensive Review Study, Final Integrated Feasibility Report and Programmatic Environmental Impact Statement*; South Florida Water Management District: Jacksonville, FL, USA; South Florida Water Management District: West Palm Beach, FL, USA, 1999; p. 4033.
57. Klimberg, R.; McCullough, B.D. *Fundamentals of Predictive Analytics with JMP*; SAS Institute: Cary, NC, USA, 2016; ISBN 1-62960-803-3.
58. Dematos, G.; Boyd, M.S.; Kermanshahi, B.; Kohzadi, N.; Kaastra, I. Feedforward versus Recurrent Neural Networks for Forecasting Monthly Japanese Yen Exchange Rates. *Financ. Eng. Jpn. Mark.* **1996**, *3*, 59–75. [CrossRef]
59. Wang, Z.; Di Massimo, C.; Tham, M.T.; Morris, A.J. A Procedure for Determining the Topology of Multilayer Feedforward Neural Networks. *Neural Netw.* **1994**, *7*, 291–300. [CrossRef]
60. Pilarz, J.; Polishuk, I.; Chorążewski, M. Prediction of Sound Velocity for Selected Ionic Liquids Using a Multilayer Feed-Forward Neural Network. *J. Mol. Liq.* **2022**, *347*, 118376. [CrossRef]
61. Ighalo, J.O.; Adeniyi, A.G.; Marques, G. Artificial Intelligence for Surface Water Quality Monitoring and Assessment: A Systematic Literature Analysis. *Modeling Earth Syst. Environ.* **2021**, *7*, 669–681. [CrossRef]
62. Najafzadeh, M.; Homaei, F.; Farhadi, H. Reliability Assessment of Water Quality Index Based on Guidelines of National Sanitation Foundation in Natural Streams: Integration of Remote Sensing and Data-Driven Models. *Artif. Intell. Rev.* **2021**, *54*, 4619–4651. [CrossRef]
63. Najafzadeh, M.; Ghaemi, A.; Emamgholizadeh, S. Prediction of Water Quality Parameters Using Evolutionary Computing-Based Formulations. *Int. J. Environ. Sci. Technol.* **2019**, *16*, 6377–6396. [CrossRef]
64. Svozil, D.; Ševčík, J.G.K.; Kvasnicka, V. Neural Network Prediction of the Solvatochromic Polarity/Polarizability Parameter. *J. Chem. Inf. Comput. Sci.* **1997**, *37*, 338–342. [CrossRef]
65. Tak, N. Meta Fuzzy Functions Based Feed-Forward Neural Networks with a Single Hidden Layer for Forecasting. *J. Stat. Comput. Simul.* **2021**, *91*, 2800–2816. [CrossRef]
66. Marini, F.; Magrì, A.L.; Bucci, R. Multilayer Feed-Forward Artificial Neural Networks for Class Modeling. *Chemom. Intell. Lab. Syst.* **2007**, *88*, 118–124. [CrossRef]
67. Rozos, E.; Dimitriadis, P.; Bellos, V. Machine Learning in Assessing the Performance of Hydrological Models. *Hydrology* **2021**, *9*, 5. [CrossRef]
68. Rasamoelina, A.D.; Adjailia, F.; Sinčák, P. A Review of Activation Function for Artificial Neural Network. In Proceedings of the 2020 IEEE 18th World Symposium on Applied Machine Intelligence and Informatics (SAMI), Herlany, Slovakia, 23–25 January 2020; pp. 281–286.
69. Conrads, P.A.; Darby, L.S. Development of a Coastal Drought Index Using Salinity Data. *Bull. Am. Meteorol. Soc.* **2017**, *98*, 753–766. [CrossRef]
70. Petkewich, M.; Lackstrom, K.; McCloskey, B.J.; Rouen, L.F.; Conrads, P.A. *Coastal Salinity Index along the Southeastern Atlantic Coast and the Gulf of Mexico, 1983 to 2018*; US Geological Survey: Reston, VA, USA, 2019.

71. McCloskey, B. *CSI: Coastal Salinity Index*; R Package Version 0.0.1: Vienna, Austria, 2022.
72. Abdi, H.; Williams, L.J. Newman-Keuls Test and Tukey Test. *Encycl. Res. Des.* **2010**, *2*, 897–902.
73. Navarro, D. *Learning Statistics with R*; Lulu.com, University of New South Wales: Kensington, Australia, 2013; ISBN 1-326-18972-7.
74. Games, P.A. Multiple Comparisons of Means. *Am. Educ. Res. J.* **1971**, *8*, 531–565. [CrossRef]
75. Frankovich, T.A.; Fourqurean, J.W. Seagrass Epiphyte Loads along a Nutrient Availability Gradient, Florida Bay, USA. *Mar. Ecol. Prog. Ser.* **1997**, *159*, 37–50. [CrossRef]
76. Marshall, F.E.; Wingard, G.L.; Pitts, P. A Simulation of Historic Hydrology and Salinity in Everglades National Park: Coupling Paleoecologic Assemblage Data with Regression Models. *Estuaries Coasts* **2009**, *32*, 37–53. [CrossRef]
77. Hudson, H.J.; Powell, G.N.; Robblee, M.B.; Smith, T.J., III. A 107-Year-Old Coral from Florida Bay: Barometer of Natural and Man-Induced Catastrophes? *Bull. Mar. Sci.* **1989**, *44*, 283–291.
78. Lorenz, J.J. A Review of the Effects of Altered Hydrology and Salinity on Vertebrate Fauna and Their Habitats in Northeastern Florida Bay. *Wetlands* **2014**, *34*, 189–200. [CrossRef]
79. Zieman, J.C. *The Ecology of the Seagrasses of South Florida: A Community Profile*; Department of the Interior, US Fish and Wildlife Service: Washington, DC, USA, 1982.
80. Barbier, E.B. Pricing Nature. In *Annual Review of Resource Economics*; Rausser, G.C., Smith, V.K., Zilberman, D., Eds.; Palo Alto: Santa Clara, CA, USA, 2011; Volume 3, pp. 337–353. ISBN 1941-1340-978-0-8243-4703-1.
81. RECOVER. *The Recover Team's Recommendations for Revisions to the Interim Goals and Interim Targets for the Comprehensive Everglades Restoration Plan: 2020. Restoration Coordination and Verification*; S. Army Corps of Engineers, Jacksonville District, Jacksonville, and South Florida Water Management District: West Palm Beach, FL, USA, 2020.
82. Marshall, F.E. The Influence of Restoration Efforts in the Freshwater Everglades on the Salinity Regime of Florida Bay. *Restor. Ecol.* **2017**, *25*, S99–S106. [CrossRef]
83. Thurig, B.; Körner, C.; Stöcklin, J. Seed Production and Seed Quality in a Calcareous Grassland in Elevated CO_2. *Glob. Change Biol.* **2003**, *9*, 873–884. [CrossRef]
84. Rae, A.M.; Ferris, R.; Tallis, M.J.; Taylor, G. Elucidating Genomic Regions Determining Enhanced Leaf Growth and Delayed Senescence in Elevated CO_2. *Plant Cell Environ.* **2006**, *29*, 1730–1741. [CrossRef]
85. Hoegh-Guldberg, O.; Bruno, J.F. The Impact of Climate Change on the World's Marine Ecosystems. *Science* **2010**, *328*, 1523–1528. [CrossRef]
86. Pearlstine, L.G.; Pearlstine, E.V.; Aumen, N.G. A Review of the Ecological Consequences and Management Implications of Climate Change for the Everglades. *J. N. Am. Benthol. Soc.* **2010**, *29*, 1510–1526. [CrossRef]
87. Catano, C.P.; Romañach, S.S.; Beerens, J.M.; Pearlstine, L.G.; Brandt, L.A.; Hart, K.M.; Mazzotti, F.J.; Trexler, J.C. Using Scenario Planning to Evaluate the Impacts of Climate Change on Wildlife Populations and Communities in the Florida Everglades. *Environ. Manag.* **2015**, *55*, 807–823. [CrossRef] [PubMed]
88. Muehllehner, N.; Langdon, C.; Venti, A.; Kadko, D. Dynamics of Carbonate Chemistry, Production, and Calcification of the Florida Reef Tract (2009–2010): Evidence for Seasonal Dissolution. *Glob. Biogeochem. Cycles* **2016**, *30*, 661–688. [CrossRef]